Comparative proteomics in the wild: Accounting for intrapopulation variability improves describing proteome response in a Gammarus pulex field population exposed to cadmium

Yannick Cogne, Christine Almunia, Duarte Gouveia, Olivier Pible, Adeline François, Davide Degli Esposti, Olivier Geffard, J. Armengaud, Arnaud Chaumot

Bisphenols disrupt differentiation of the pigmented cells during larval brain formation in the ascidian

Isa D.L. Gomes[a,*], Ievgeniia Gazo[a,b], Dalileh Nabi[a#], Lydia Besnardeau[a], Céline Hebras[a], Alex McDougall[a], Rémi Dumollard[a,*]

[a]Laboratoire de Biologie du Développement de Villefranche-sur-mer (LBDV) UMR7009, Sorbonne Universités, Université Pierre-et-Marie-Curie, CNRS, Institut de la Mer de Villefranche (IMEV), Villefranche-sur-mer, France
[b]University of South Bohemia in Ceske Budejovice, Faculty of Fisheries and Protection of Waters, Research Institute of Fish Culture and Hydrobiology, Laboratory of Molecular, Cellular and Quantitative Genetics, Zátiší 728/II, 389 25, Vodňany, Czech Republic

* Corresponding authors: remi.dumollard@obs-vlfr.fr; igobio12@gmail.com
# Current address: Medical Theoretical Center, TU-Dresden, Fiedlerstrasse 42, D-01307 18 Dresden, Germany

Abstract

The endocrine disruptor Bisphenol A (BPA), a widely employed molecule in plastics, has been shown to affect several biological processes in vertebrates, mostly via binding to nuclear receptors. Neurodevelopmental effects of BPA have been documented in vertebrates and linked to neurodevelopmental disorders, probably because some nuclear receptors are present in the vertebrate brain. Similarly, endocrine disruptors have been shown to affect neurodevelopment in marine invertebrates such as ascidians, mollusks or echinoderms, but whether invertebrate nuclear receptors are involved in the mode-of-action is largely unknown.

In this study, we assessed the effect of BPA on larval brain development of the ascidian *Phallusia mammillata*. We found that BPA is toxic to *P. mammillata* embryos in a dose-dependent manner (EC_{50}: 11.8µM; LC_{50}: 21µM). Furthermore, micromolar doses of BPA impaired differentiation of the ascidian pigmented cells, by inhibiting otolith movement within the sensory vesicle. We further show that this phenotype is specific to other two bisphenols (BPE and BPF) over a bisphenyl (2,2 DPP). Because in vertebrates the estrogen-related receptor gamma ($ERR\gamma$) can bind bisphenols with high affinity but not bisphenyls, we tested whether the ascidian ERR participates in the neurodevelopmental phenotype induced by BPA. Interestingly, *P. mammillata* ERR is expressed in the larval brain, adjacent to the differentiating otolith. Furthermore, antagonists of vertebrate ERRs also inhibited the otolith movement but not pigmentation. Together our observations suggest that BPA may affect ascidian otolith differentiation by altering *Pm*-ERR activity whereas otolith pigmentation defects might be due to the known inhibitory effect of bisphenols on tyrosinase enzymatic activity.

Keywords:
Ascidian, Bisphenol A, Estrogen-related receptor, Invertebrate, Neurodevelopment, Otolith

Abbreviations:
BPA: bisphenol A; DES: diethylstilbestrol; ED: endocrine disruptor; ERR: estrogen-related receptor; E2B: 17β-estradiol 3-benzoate; NR: nuclear receptor; PC: pigmented cells; 4OHT: 4-hydroxytamoxifen

1. Introduction

Bisphenol A (BPA), a well-known molecule used in plastics, was considered harmless to human health until Krishnan and colleagues found that it could easily leach from plastics into their yeast cultures (Krishnan et al. 1993). BPA was later found accidently to be a potent meiotic aneugen in mouse females (Hunt et al. 2003). Because BPA is continuously released into the environment, human and wildlife are ubiquitously exposed despite its short half-life, making BPA a pseudo-persistent chemical (Flint et al. 2012). Consequently, concerns have been raised about BPA due to its potential endocrine disrupting activities. Endocrine disruptors (EDs) are compounds able to mimic hormones and interfere with different biological processes (Gomes et al. 2019; Schug et al. 2016).

In vertebrates, BPA has several targets such as membrane receptors like G protein-coupled estrogen receptor 1 (GPER), the aryl hydrocarbon receptor (AhR), or several nuclear receptors such as Estrogen Receptor (ER), Estrogen-Related Receptor (ERR), Peroxisome Proliferator-Activated Receptor (PPAR), Pregnane X Receptor (PXR) and Thyroid Receptor (TR) (Delfosse et al. 2014; Acconcia et al. 2015; Murata and Kang 2017; Mackay and Abizaid 2018). While disruption of steroid and thyroid systems by EDs have been associated with the presence of nuclear receptors in the reproductive system and thyroid (ER, AR, TR), the discovery of nuclear receptors presence in the vertebrate brain (ER, ERR, PPAR and PXR) lead researchers to suspect about the potential hazard of EDs to vertebrate neurodevelopment and to link these chemicals with an increase of neurodevelopmental disorders (Inadera 2015; Mustieles et al. 2015; Braun 2017; Nesan et al. 2017).

Previous reviews have shown that invertebrate development can also be affected by BPA (Flint et al. 2012; Canesi and Fabbri 2015; Dumollard et al. 2017). Studies indicate that BPA may be harmful to wildlife even at environmentally relevant concentrations (0.05µM or lower) (Flint et al. 2012). The highest concentration found in natural surface waters was 0.1µM, but landfill leachates from municipal wastes registered BPA concentrations around 75µM (Flint et al. 2012). Even though the toxicity of BPA has been described and studied in invertebrates, there is a lack of knowledge concerning its mode-of-action, including BPA's impact on neurodevelopment (Kaur et al. 2015; Mersha et al. 2015; Dumollard et al. 2017; Messinetti et al. 2018a; Messinetti et al. 2018b). Because invertebrate embryos do not possess a circulatory system (transporting hormones), nuclear receptors are the most likely targets for endocrine disruption as they are found in all marine invertebrates, from marine sponges to ascidians (Holzer et al. 2017). Yet, roles of most nuclear receptors (NRs) in invertebrates are still poorly known and efforts are being made to fill this gap (Gomes et al. 2019; Markov and Laudet 2011; Holzer et al. 2017). Unlike vertebrates, other mechanisms of toxicity (membrane receptors, oxidative stress, epigenetics) are completely unknown in invertebrates and they are not as conserved as NR signaling is (Gomes et al. 2019; Holzer et al. 2017).

Ascidians (Tunicata) are marine invertebrate chordates. Upon fertilization, the ascidian embryo develops into a larva that shows a prototypical chordate body plan (Hudson 2016) within only 18 hours (Hotta et al. 2007). The brain of the ascidian larva is located in the trunk and is composed by an anterior sensory vesicle and a trunk ganglion (Gomes et al. 2019), and expresses typical specification markers such as Cnga, Coe, Islet, Pax6, among others (Hudson 2016). In the sensory vesicle, two pigmented cells (PC) are visible, the otolith and the ocellus. The otolith (Ot), responsible for gravity sensing, is an unicellular structure which has a free part within the lumen of the sensory vesicle and a ventral foot part (Dilly 1962; Esposito et al. 2015). The ocellus (Oc), involved in light perception, was previously described as a multicellular structure made up of one pigmented cell, three lens cells and 37 photoreceptor cells (Dilly 1964; Ryan et al. 2016). Specification process of the PC starts at late gastrula (stage 13) by the induction of specific genes such as tyrosinase (Tyr), tyrosinase-related proteins (Tyrp1/2a, Tyrp1/2b) and the GTPase Rab32/38 (Nishida and Satoh 1989; Racioppi et al. 2014). At late neurula (st. 16), PC specification ends and differentiation starts. While the gene regulatory network (GRN) involved in ascidian PC specification is well characterized, the GRN involved in PC differentiation is not known. Recent studies in ascidians showed that BPA affects neurodevelopment by disrupting the pigmented cells and GABAergic and dopaminergic neurons, and it was even suggested that the ascidian nuclear receptor ERR might be involved in the toxic mode-of-action of BPA (Messinetti et al. 2018b; Messinetti et al. 2018a). Nevertheless, phenotype of BPA on ascidian PC is still poorly characterized and the presence of ERR in the ascidian embryo is currently unknown.

In this study, we assessed the effect of BPA on brain development of the ascidian larva (*Phallusia mammillata*). By imaging PC behavior and analyzing gene expression in the forming ascidian brain, we found that BPA at lower doses specifically impaisr PC development by disrupting otolith pigmentation and differentiation. We further show that this phenotype is also induced by bisphenol E and bisphenol F but not by a bisphenyl or estradiol. Because in vertebrates ERRγ has been shown to bind bisphenols but not bisphenyls, and due to previous reports on ERR implication in zebrafish otolith development (Tohmé et al. 2014), we decided to test if the ascidian ERR could be mediating BPA toxicity. We found that *P. mammillata* ERR is expressed in the ascidian sensory vesicle during PC differentiation and ERR antagonists partially copied BPA phenotype, suggesting that it might participate in the neurodevelopmental effect of BPA in the ascidian larva.

2. Material and Methods

2.1. Animals

Phallusia mammillata adults were collected in Sète (Hérault, France), and kept at 17±1ºC in circulating seawater aquaria. They were reared under constant light conditions to avoid uncontrolled spawning of eggs and sperm (Lambert and Brandt, 1967). The animals were kept and maintained by the *Centre de Ressources Biologiques Marines* of the institute (CRBM - IMEV).

For exposure experiments, eggs and sperm were collected separately by dissecting the gonoducts of several hermaphrodite adults. Sperm was stored at 4°C, while eggs were placed in natural filtered (0.2 µm) seawater (FSW) supplemented with TAPS buffer (0.5 mM) and EDTA (0.1 mM) (Sardet et al. 2011). To allow fluorescence microscopy analysis, chorion was removed from eggs by incubating in a trypsin solution for 2 hours, and then washed 3 times before use (McDougall et al. 2015). Eggs were fertilized by incubating them with a sperm dilution (1:100) for 10 min, then washed 3 times and left in filtered seawater (FSW/TAPS/EDTA) at 18°C until the desired developmental stage. Since *Phallusia mammillata* development is very similar to *Ciona robusta*, all referred developmental stages are based on published *Ciona* development (Hotta et al. 2007). Please refer to figure 2D for general ascidian developmental stages and figure 2A for specific brain developmental stages. The details of all protocols for embryos handling can be found online at http://lbdv.obs-vlfr.fr/fr/ascidian-biocell-group.html .

2.2. Chemical products

For embryo culture, TAPS buffer (CAS Nr. 29915-38-6) and EDTA (CAS Nr. 60-00-4) were used. For toxicity studies, the following chemicals were diluted in dimethyl sulfoxide (DMSO, CAS Nr. 67-68-5): Bisphenol A (BPA, CAS Nr. 80-05-7), Bisphenol E (BPE, CAS Nr 2081-08-5), Bisphenol F (BPF, CAS Nr 620-92-8), Diethylstilbestrol (DES, CAS Nr 56-53-1), Phenylthiourea (PTU, CAS Nr. 103-85-5), UO126 (CAS Nr. 109511-58-2), β-Estradiol 3-benzoate (E2B, CAS Nr 50-50-0), 2,2-Diphenylpropane (2,2DPP, CAS Nr 778-22-3), 4-Hydroxytamoxifen (4OHT, CAS Nr 68392-35-8). For F-actin and DNA staining, phalloidin-tetramethylrhodamine B isothiocyanate (Phalloidin-TRITC, Santa Cruz Biotechnology) and Hoechst (CAS Nr. 23491-52-3) were used, and samples conserved with Citifluor AF1 antifade mounting solution (Biovalley). All chemicals were purchased from Sigma Aldrich, unless stated otherwise.

2.3. Exposure experiments

Exposure experiments with BPA, BPE, BPF, 2,2 DPP, E2B, DES, 4OHT and PTU were performed in the same way. Chemicals were dissolved in DMSO to have a 0.5 M main stock solution. After fertilization, stage 1 embryos were transferred to chemical-containing seawater (FSW-TAPS-EDTA). Due to a possible confusion arising from differences in the concentrations of DMSO, each solution was diluted in DMSO to a concentration 10,000 times higher than required, and again diluted in filtered seawater (1:10000), giving the required concentration of chemical in an overall solution of 0.01% DMSO in seawater. As a control treatment, 0.01% DMSO seawater was used.

For the exposure experiment with UO126, the chemical was dissolved in a 0.04 M DMSO stock solution. Embryos were fertilized and left to develop at 18°C until stage 16. Embryos were then exposed at stages 16 and 18, at a final concentration of 4 µM defined from a previous study (Racioppi et al. 2014). A control treatment with 0.01% DMSO was performed.

At stage 26, larvae were fixed in 4% paraformaldehyde (4% PFA, 0.5 M NaCl, PBS; Sigma), washed 3 times in Phosphate Buffered Saline (PBS 1X) and imaged by light microscopy (*Zeiss Axiovert 200*) at 10x magnification. Each experiment was replicated at least 3 times.

2.4. Embryo morphology analysis

For general morphology analysis, larvae (st. 26) were analyzed by scoring the percentage of normal (good general embryo morphology, with proper trunk and palps formation, as well as tail elongation), malformed (embryos with bent tail) and not developed embryos (with arrested development before gastrulation/tail extension) (see figure 1). Statistical analysis was performed as described in section 2.11.

For trunk morphology analysis, the area of each PC (*PC area*, μm^2), the distance between the two PCs (*PC distance*, µm) and the length and width of the trunk were measured and transformed in a ratio (Trunk L/W ratio) (see figure 2A). The morphological analysis was performed using *Toxicosis*, a software developed in our laboratory (*IDDN.FR.001.330013.000.S.P.2018.000.10000*, deposited on July 13th 2018). The resulting data was normalized to each respective control treatment (100%) and plotted in radar charts for better comparison of phenotypes between chemicals. Statistical analysis was performed as described in section 2.11. Please note that only exposure experiments with control treatments showing a mean PC area equal or superior to 300 μm^2 and a percentage of undeveloped embryos lower than 20% were suitable for further analysis.

2.5. BPA time-window action

To assess the time-window action of BPA during *Phallusia mammillata* embryogenesis, embryos were incubated in BPA-containing seawater at different times during embryogenesis. In a first phase, embryos were exposed in three different ways: 1) six hours before fertilization (6 *hbf*), 2) six hours after fertilization (6 *hpf*, time to reach gastrulation, i.e. stage 10), or 3) both before and after fertilization (from stage 0 to 10) for a total of 12 hours BPA exposure (please refer to diagram on figure 2D). Embryos were then washed and incubated in FSW/TAPS/EDTA up to stage 26. In a second phase, embryos were exposed at different stages (10, 12, 14, 16, 18 and 20) until stage 26. At stage 26, embryos from all treatments were fixed (4% PFA) for later analysis of pigment cell area (*PC area*, μm^2). For a matter of technical feasibility, embryos were cultured at 14°C from fertilization to stage 16 and then placed at 18°C from stage 16 to stage 26. Statistical analysis was performed as described in section 2.11.

2.6. Immunofluorescence

To assess the effect of BPA on mitotic spindle formation, microtubule organization during the first mitosis was assessed. For this, eggs were fertilized and immediately exposed to 0.01% DMSO or BPA 40 µM. Sixty-four minutes after fertilization (during the first mitosis), embryos were fixed in cold 100% methanol overnight. They were then progressively rehydrated in PBS/0.02%Triton, permeabilized in PBS/0.25%Triton for 15 min at RT, and then incubated in primary and secondary antibodies in PBS/1%BSA overnight at 4°C (for each antibody incubation, fixed embryos were washed for 15 min for 4 times with PBS/0.1%Tween). Fixed embryos were stained for microtubules with primary antibody anti-α-tubulin (DM1A; Sigma-Aldrich 1:1000) and mouse FITC secondary antibody (Jackson) diluted 1:50. To stain DNA, immunofluorescence labelled embryos were mounted in VectaShield that contains DAPI (Vector Laboratories) analyzed with epifluorescence microscopy (40X objective, *Zeiss Axiovert 200*).

Cilia in the neurohypophysial duct and neural tube were assessed by immunostaining with anti-acetylated α-tubulin antibody according to previously published protocols (Sardet et al. 2011). Stained larvae were imaged by confocal microscopy (Leica, SP8).

2.7. Analysis of otolith movement by timelapse imaging

To follow otolith development, eggs were injected with reporter plasmids bearing promoter region for *Ciona* genes driving the expression of GFP based reporters. The promoters used are Tyrosinase-related protein (pTyrp, kind gift from Filomena Ristoratore), ßγCrystallin (pßγC, kind gift from Philip Abitua) and Muscle segment homeobox (pMsx, kind gift from Philip Abitua) to visualize pigment cell precursors. The GFP-based reporters were either Venus/Cherry (cytosolic), H2B::Venus/Cherry (DNA) or Lifeact::Venus/Cherry (actin-rich cell cortex). To visualize the plasma membrane of all cells mRNAs coding for PHdomain::Tomato was injected

in unfertilized eggs as previously described (McDougall et al. 2015). Injected eggs were fertilized 2 hours after injection and left to develop until stage 10 (gastrula). Then, embryos were either transferred to 0.01% DMSO (figure 3A) or to BPA-containing seawater (10 µM, figure 3B) and at stage 20 (early tailbud) embryos were mounted on a slide for time-lapse live imaging using confocal microscopy (Leica SP8).

2.8. Analysis of otolith foot by Phalloidin staining

To analyze the otolith foot structure, embryos were exposed to BPA analogues BPE, BPF and 2,2 DPP (section 2.3). Once at the desired stage (st. 26), embryos were fixed with 4% PFA overnight at 4°C. Embryos were washed twice with PBS 1X, incubated in PBS-BSA solution (3% BSA diluted in PBS 1X) for 1h and stained with Phalloidin-TRITC and Hoechst diluted 1:500 in PBS-BSA, for 3h at RT. Embryos were washed twice in PBS-BSA, once in PBS and stored in AF1 antifade mounting solution Citifluor (Biovalley) until analysis. Phenotypes were compared to a control treatment (0.01% DMSO) using confocal microscopy (Leica SP8). Please note the same final concentration was used for all molecules (10µM), with the exception of 2,2DPP (25µM), since no phenotype was visible at 10µM, 25µM nor 100µM.

2.9. mRNA expression pattern analysis by *in situ* hybridization (ISH)

mRNA expression patterns of *Phallusia mammillata* genes were assessed by *in situ* hybridization (ISH) technique. For this, embryos were fixed overnight at 4°C (ISH fix: 4% formaldehyde, 100 mM MOPS, 0.5 M NaCl, pH 7.6), washed in PBS, dehydrated in ethanol and stored at –20°C until analysis. *Phallusia* ISH was performed as previously described (Paix et al. 2009).

ISH probes covering the entire cDNAs were designed based on *Aniseed* (http://www.aniseed.cnrs.fr/) and *Octopus* (http://octopus.obs-vlfr.fr/index.php) databases and were obtained from the *Phallusia mammillata* cDNA library (pExpress-1 vector based) available in our laboratory. After amplification by PCR and confirmation by electrophoresis, PCR products were purified (Qiagen MinElute PCR purification kit, Qiagen) and DNA quantified. Digoxygenin-labeled antisense RNA probes (DIG RNA Labeling Mix, Roche) were then prepared and detection was based on NBT/BCIP (Roche) principle. The following genes were assessed: Tyr (gene ID: *Phamm.g00005364*), Rab32/38 (gene ID: *Phamm.g00006935*), Pax6 (gene ID: *Phamm.g00010911*), Cnga (gene ID: *Phamm.g00015101*), Coe (gene ID: *Phamm.g00012706*) and Islet (gene ID: *Phamm.g00000576*). The imaging of all embryos was performed using bright field microscopy (*Zeiss Axiovert 200*).

2.10. Estrogen-Related Receptor embryonic expression

The sequence for *Phallusia mammillata* ERR (*Pm*-ERR) is published on *Aniseed* database (gene ID: *Phamm.g00012306*) and was cloned from *Phallusia mammillata* cDNA library and processed by ISH as described in section 2.9.

2.10.1. *Pm*-ERR gene activity by promoter cloning

Gene activity was assessed by cloning the promoter region of *Pm*-ERR into a vector driving the expression of a GFP reporter. For this, a 1.7 kbp fragment (-1705 from the Transcription Start Site, *TSS*, figure 6C) was selected from ascidian genome available on *Aniseed* database. This region, which is highly conserved with *Phallusia fumigata*, was amplified by PCR from *P. mammillata* genomic DNA and cloned upstream a H2B::Venus reporter by In-Fusion HD Cloning Plus kit (Takara Bio). The prepared construct (pERR>H2B::Venus) was microinjected in *P. mammillata* eggs and the transgenic embryos analyzed by confocal imaging (Leica TCS SP8).

2.10.2. *Pm*-ERR protein levels analyzed by a specific antibody against *Pm*-ERR

To determine protein presence by immunoblot, an antibody against the ERR protein was made by producing the protein and sending it to Covalab (France) to immunize mice. Four anti-serum were screened and results from the most reactive anti-serum are shown. The anti-serum was further validated as described in figure 6D. In order to confirm the antibody specificity, the antibody was tested against exogenous *Pm*-ERR (*Pm*-ERR::Venus mRNA injected larvae).

2.11. Statistical analysis

All presented data show mean with error bars indicating standard deviation (mean±SD). The number of embryos (*n*) analyzed for each graph is indicated in the figure legend. For figure 2C and figure 6, descriptive statistics is depicted in table I. For figure 2D, *n* and *P values* are indicated in the figure legend.

GraphPad Prism® software (GraphPad Software, Inc. CA, USA) was used to calculate median lethal (LC_{50}) and effective (EC_{50}) concentrations, as well as to perform analysis of variance (α=0,05) to evaluate differences between treatments. Since data did not follow a Gaussian distribution (Shapiro-Wilk normality test), nonparametric Kruskal-Wallis test was performed and statistical differences between control and treatments were assessed by Dunnett's test.

3. Results

3.1. Bisphenol A is toxic to *P. mammillata* embryos in a dose-dependent manner

Figure 1 shows the effect of BPA on the general morphology of *Phallusia* embryos after 24 hours of exposure. Embryos of *P. mammillata* were exposed to different concentrations of BPA (from 100 nM to 30 µM) and a significant increase in malformed and not developed larvae was observed from 10 µM BPA (compared to the control treatment 0.01% DMSO, ANOVA - Dunnett's Multiple Comparison Test: $p<0.05$, figure 1). At 15 µM and 20 µM larvae were mostly malformed (60% and 65%, respectively), and at 25 and 30 µM larvae were mostly not developed (95% and 100%, respectively). Observation of the mitotic spindle in one cell embryos exposed to 40 µM BPA showed a severe disruption of mitotic spindle in BPA exposed embryos compared to controls (fig S1) suggesting that at this dose BPA acts as an aneugenic genotoxic. No visible effect was detected when embryos were exposed to nanomolar concentrations. BPA median effective (EC_{50}, malformed) and lethal (LC_{50}, not developed) concentrations for *P. mammillata* embryogenesis were 11.8 µM and 21 µM, respectively.

3.2. Bisphenol A induces neurodevelopmental toxicity in *P. mammillata* embryos

Careful observation revealed that at 10 µM of BPA, within embryos showing normal overall morphology with proper trunk and tail elongation (figure 1), the pigmented cells (PC) within the sensory vesicle were strongly affected. In order to better describe the phenotype of BPA, formation of sensory vesicle was recorded by timelapse imaging of embryonic development between stage 21 (early tailbud) and stage 26 (hatching larva) (figure 2A, 2B), during which differentiation of the sensory vesicle and pigmented cells occurs (Esposito et al. 2015).

In non-exposed embryos (0.01% DMSO, figure 2A), the first pigments appear at stage 21 (black arrowhead), increasing at stage 22. At stage 23 adhesive palps start to protrude (yellow arrowhead) and two distinct PC are visible: the ocellus (*Oc*, blue arrowhead) and the otolith (*Ot*, pink arrowhead). At this stage, a lumen is first visible in the sensory vesicle (orange arrowhead) and this lumen expands until stage 26. At stage 25, the trunk begins to elongate and concomitantly the otolith moves towards the ventral side of the sensory vesicle. Finally, at stage 26, larvae display two clearly separated PC and palps, as well as an elongated trunk. Note that pigmentation, otolith movement and other events happen concomitantly.

When comparing to non-exposed embryos, embryos exposed to BPA at stage 1 (BPA 10 µM) clearly showed a reduction of pigmentation and a blocked otolith movement towards the ventral side of the sensory vesicle (figure 2B). Additionally, both sensory vesicle lumen (svl) formation and trunk elongation seemed slightly reduced. Palps were the only well-formed structures when compared to non-exposed embryos. We then quantified pigmentation by measuring the area of both PC (PC area); the otolith movement by measuring the distance between PC (PC distance); and the trunk by measuring the length and width (Trunk L/W ratio). BPA-exposed embryos showed significant reduction for all the three endpoints (ANOVA - Dunnett's Multiple Comparison Test: p-value<0.001; table I), with PC area reduced to 35%, PC distance reduced to 31% whereas Trunk L/W ratio was less affected (reduced to 70%) (figure 2C). Additionally, the sensory vesicle lumen seemed also reduced but this was not quantified.

In order to understand the window of action of BPA on pigmented cells formation, embryos were incubated at different times during embryogenesis (figure 2D). Reduction of pigmentation (PC area) was always observed when BPA was present between stage 10 and stage 26 (ANOVA - Dunnett's Multiple Comparison Test: p-value<0.001), and not when it was washed before stage 10. Strikingly, reduced pigmentation was still

observed when BPA was added as late as stage 20. We also exposed eggs to BPA before fertilization (stages 0-1 and 0-10) to assess whether bioaccumulation of BPA could influence the phenotypes observed. However, even when BPA was allowed to accumulate for 6-12 hours and washed out at stage 10, no effect on pigmentation was observed.

In *Ciona*, the formation of the pigmented cells necessitates tyrosinase activity for the pigmentation of melanosomes (Caracciolo et al. 1997) and FGF/MAPK signals up to stage 16 for specification (Racioppi et al. 2014). Accordingly, *Phallusia* embryos exposed to the tyrosinase enzyme inhibitor phenylthiourea (PTU, from 1-cell stage (Whittaker 1966; Sakurai et al. 2004)) resulted in the complete lack of pigmented melanosomes in the PC, but the unpigmented otolith cell seemed well formed and ventrally placed in the sensory vesicle lumen (figure S2A). The phenotype obtained is clearly different from the phenotype induced by application of BPA at a similar timing (figure 2B).

Moreover, embryos exposed to the MAPK inhibitor UO126 at stage 16 are completely devoid of PC and sensory vesicle lumen, whereas embryos treated with UO126 at stage 18 display two well separated PC and normal sensory vesicle lumen (figure S2A). Once again, the phenotypes induced by MAPK inhibition are different from the observed BPA phenotype. In addition, spatial expression of Tyr, Rab32/38, Pax6, Cnga, Coe and Islet genes, known to be necessary for PC and/or CNS specification, was analyzed by *in situ* hybridization (ISH) (figure S2B). No differences in the spatial expression patterns between non-exposed (DMSO) and BPA-exposed embryos (BPA 10µM) were observed, suggesting that BPA does not affect PC nor CNS specification. Finally, differentiation of the neurohypophysial duct and neural tube (Konno et al. 2010) was not affected by BPA as shown in figure S2C, reinforcing the idea that only PC differentiation is affected by BPA exposure.

3.3. Bisphenol A impairs otolith cell movement towards the ventral side of the sensory vesicle

We have observed so far that BPA affects processes intervening in sensory vesicle differentiation between stage 21 and 26. In order to characterize with more precision, we performed time-lapse imaging of embryos expressing fluorescent-tagged reporters in the pigmented cells (PC) lineage. By using the otolith specific promoter (pßγC::GFP) we could clearly observe changes in the shape of the otolith between stage 21 (when it is in the epithelium of the sensory vesicle) and stage 25 (when the otolith is bulging into the sensory vesicle lumen and contacts the sensory vesicle epithelium by a foot structure) (figure 3A). The actin network of PC was specifically visualized with a PC specific promoter (pTyrp>LifeAct::3xVenus) together with bright field imaging. Timelapse imaging shows that the otolith cell detaches its foot from the dorsal sensory vesicle epithelium (and from the ocellus) at stage 26, moving towards the ventral side of the sensory vesicle epithelium (figure 3B and supplementary movie 1). Note that the sensory vesicle lumen also expands during these stages. In BPA-exposed embryos, the otolith cell still forms its foot but it does not detach from the dorsal sensory vesicle epithelium, remaining tethered to the ocellus. In addition, expansion of the sensory vesicle lumen seems to be reduced (figure 3C and supplementary movie 2).

We then assessed whether this phenotype is specific to bisphenol A, by exposing embryos to BPE and BPF (two other bisphenols) and 2,2DDP (a bisphenyl) (figure 4A). For this, exposed larvae (stage 26) were stained with Phalloidin and Hoechst to visualize both actin and DNA structures. The control larvae (0.01% DMSO, figure 4B) showed an accumulation of actin abutting the otolith foot on the ventral side of the sensory vesicle. In contrast BPA-exposed larvae displayed a dorsal/posterior otolith actin-rich foot (figure 4C). Interestingly, both BPE and BPF exposures resulted in the presence of the otolith actin-rich foot in the dorsal side of the sensory vesicle (figures 4D and 4E), suggesting that otolith movement did not occur. Finally, exposure to 25µM 2,2 DPP did not affect the localization of the otolith foot which was still observed on the ventral side of the sensory vesicle (figure 4F), suggesting that the bisphenyl does not affect otolith movement. No phenotype was observed with either 10 or 100µM 2,2 DPP (data not shown). Even though we did not quantify it, BPE and BPF (but not 2,2 DPP) also seem to decrease PC pigmentation and sensory vesicle lumen expansion (compare the different larvae shown in figures 4B-F). Because bisphenols but not bisphenyl have been previously shown to bind human Estrogen-Related Receptor (ERR) with high affinity (see Discussion), we thus sought for ERR presence in *P. mammillata* larvae.

3.4. Estrogen-Related Receptor (ERR) is expressed in *Phallusia mammillata* larvae

In order to substantiate the possibility that BPA targets ERR in the ascidian embryo, we analyzed ERR transcripts and protein level during embryonic development (figure 5). Published transcriptomic data in the ascidian *Aniseed* database suggests that ERR transcripts are found at larvae (stage 26) but not before (Gomes et al. 2019). ISH analysis revealed that, at stage 26, ERR is expressed within the sensory vesicle, more precisely above the ocellus, between otolith and ocellus and underneath the otolith, as well as in adhesive palps and trunk ganglion (figure 5A, black arrowheads). Since ISH staining using NBT/BCIP at such a late stage is made difficult by the secretion of the ascidian tunic (larvae become dark quickly), we further confirmed ERR zygotic expression by monitoring its promoter activity (pERR>H2B::Venus) in transgenic embryos (Stolfi and Christiaen 2012) (figure 5B). On the 20 injected larvae, all showed fluorescent nuclei (i.e. promoter activity) in the sensory vesicle, with 13 having additional cells in the adhesive palps, while the other 7 had additional cells in the trunk ganglion. Additionally, 2 larvae showed ectopic expression in the mesenchyme due to promoter leakiness previously reported in ascidians (Stolfi and Christiaen 2012).

Using an antibody specific for *Pm*-ERR (figure 5C), ERR protein levels were measured during development by western blot analysis (figure 5D). As expected from transcriptomic data available from the ascidian database *Aniseed*, ISH and promoter analysis, a strong band (≈ 50 kDa) was observed at stage 26 but not before.

3.5. ERR antagonists also affect PC development

BPA is known to bind both ERα and ERβ and also ERRγ in vertebrates (Takayanagi et al. 2006). We thus exposed embryos to the ER agonist β-Estradiol 3-benzoate (E2B) and to the ERR antagonists diethylstilbestrol (DES) and 4-hydroxytamoxifen (4OHT). These ERR antagonists were selected as they have been shown to inhibit ERR from another ascidian species (*Halocynthia roretzi*) by transactivation assays in a human cell line (Park et al. 2009). Effect of E2B, DES and 4OHT on PC differentiation and trunk elongation was assessed. Figure 6 shows radar chart plotting of the relative differences in three measured endpoints (PC area, PC distance and Trunk L/W ratio) between control and exposed embryos, in order to compare the phenotypes induced by the different molecules.

As expected (see Discussion), the ER agonist E2B did not affect any endpoint measured (figure 6A, table I). Regarding PC differentiation, the PC distance was significantly reduced by both ERR antagonists, although to a lesser extent than BPA (figures 2C, 6B and 6C; table I; BPA 10µM: 31%, DES 1µM: 65%, 4OHT 10µM: 58%). The trunk elongation was also affected in similar proportions with BPA (figures 2C, 6B and 6C; table I; BPA 10µM: 70%, DES 1µM: 75%, 4OHT 10µM: 75%). Finally, PC area was not significantly affected by DES (figure 6B and table I; DES 1µM: 101%) nor by 4OHT (figure 6C and table I; 4OHT 5µM: 98%, 10µM: 105%), contrarily to BPA (figure 2C and table I; BPA 10µM: 35%). Please note that the concentration of DES used (1µM) was relatively low compared to BPA or 4OHT (5µM-10µM) due to the fact that embryos showed high sensitivity to DES (100% undeveloped embryos at 2µM, data not shown).

Our pharmacological screen shows that ERR antagonists can partially reproduce the phenotype of BPA, by affecting the PC distance, i.e., the otolith movement within the sensory vesicle, but not the pigmentation process.

4. Discussion

BPA has been shown to affect multiple targets and may have diverse and pleiotropic modes-of-action. Moreover, embryonic development has been shown to be one of the most critical windows of action for EDCs, particularly during neurodevelopment (Heyer and Meredith 2017). In our study we show that BPA acts during a precise window of the ascidian embryonic development, disrupts the pigmentation process and specifically blocks otolith movement within the sensory vesicle. A pharmacological approach suggests that the observed phenotype may be specific to bisphenols (BPE, BPF) over a bisphenyl (2,2 DPP). Finally, we hypothesize that the effect of BPA on ascidian larval brain formation may be mediated by ERR as suggested by a screen of ERR antagonists and the zygotic expression of ERR in a few cells of the sensory vesicle.

4.1. Bisphenol A is toxic to ascidian embryos

Phallusia mammillata embryos display a dose-dependent sensitivity to BPA with a common monotonic dose-response curve. Moreover, in our study BPA was shown to affect *P. mammillata* pigmented cells, in a similar way as recently published (Messinetti et al. 2018a), as well as in another ascidian species, *Ciona robusta* (Matsushima et al. 2013; Messinetti et al. 2018b). However, because of variability of the neural phenotypes reported before (Messinetti et al. 2018a), we performed a quantitative analysis of brain formation to better define BPA phenotype.

Concerning dose-response toxicity, our data indicates that *P. mammillata* embryos are less sensitive to BPA (EC_{50}: 11.8µM; LC_{50}: 21µM) than other marine invertebrates like the ascidian *Ciona robusta* (EC_{50}: 0.7µM; LC_{50}: 5.4µM (Matsushima et al. 2013); LC_{50}: 5.2µM (Messinetti et al. 2018b)) or the sea urchin *P. lividus* (LC50: 3.1µM (Ozlem and Hatice 2007)), but more sensitive than the vertebrate zebrafish (EC_{50}: 25µM; LC_{50}: 73.4µM (Tse et al. 2013)), even though all the referred EC_{50}/LC_{50} values are within the micromolar range. At higher dose (40µM, figure S1) BPA clearly act as an aneugen by disrupting mitotic spindle formation, as previously described in other invertebrate species like *C. elegans* (Allard and Colaiacovo 2010) and sea urchin (George et al. 2008).

4.2. Bisphenols specifically alter differentiation of the ascidian pigmented cells

In addition, our study reveals that BPA exerts neurodevelopmental toxicity by disrupting the differentiation of the ascidian pigmented cells. Neurodevelopmental defects induced by BPA have been found in vertebrates (mouse, fish, frog, reviewed in Inadera 2015; Nesan, Sewell, and Kurrasch 2017) and in invertebrates such as *Drosophila* (Kaur et al. 2015), *C. elegans* (Mersha et al. 2015), *P. mammillata* (Messinetti et al. 2018a) and *Ciona robusta* (Messinetti et al. 2018b). Time-lapse live imaging of the transparent *Phallusia* embryos allowed us to describe in detail the differentiation of pigmented cells occurring in the ascidian brain (Racioppi et al. 2014; Esposito et al. 2015) and how it is affected by BPA.

One of the main events affected by BPA was pigmentation. Several studies described pigmentation problems caused by BPA both in invertebrates and vertebrates. Concerning invertebrates, a similar phenotype was observed in another *P. mammillata* study (Messinetti et al. 2018a) and in *C. robusta* (Messinetti et al. 2018b), where both ocellus and otolith were severely affect by BPA, either characterized by reduced, supernumerary or a total absence of pigmented cells. In vertebrates, the pigmentation process consists in the production of melanin pigments and later storage in melanosomes. Pigmentation in vertebrates is mostly regulated by microphthalmia-associated transcription factor (MITF) and dependent on proteins such as tyrosinase (Tyr), tyrosinase-related proteins (Tyrp) and Rab GTPases (Wasmeier et al. 2008). In *Ciona*, PC specification is also dependent on Mitf, Tyr, Tyrp and Rab32/38 (Abitua et al. 2012; Racioppi et al. 2014), regulated under several FGF/MAPK signals from stage 13 up to stage 16 (Racioppi et al. 2014). In our study, the window of action of BPA (i.e. after stage 20) is after the final FGF-mediated induction of PC lineage (at stage 16), suggesting that BPA is affecting PC differentiation rather than PC specification. Several observations confirmed that PC specification is not affected by BPA. First, inhibiting PC specification by timed inhibition of MAPK signaling (using UO126) did not phenocopy BPA phenotype. Second, several marker genes for PC and CNS specification in ascidians (Tyr, Rab32/38, Pax6, Cnga, Coe and Islet) are not affected by BPA exposure. Altogether, our data reinforces the idea that BPA is not acting at the PC specification level, but most likely during PC differentiation. However, the gene regulatory networks involved in ascidian PC differentiation are not known and thus more efforts are needed to assess the potential genes that are being affected by BPA.

The otolith movement within the sensory vesicle was another clear effect after BPA exposure, resulting in a shorter distance between the ocellus and the otolith. By imaging transgenic *Phallusia* embryos expressing GFP markers in the PC lineage (*Tyrp*, *ßγCrystallin* and *Msx*), it was possible to visualize that the otolith cell changes shape and protrudes into the sensory vesicle lumen, which is enclosed by the sensory vesicle epithelium. The otolith cell assumes a round shape at the beginning of PC differentiation, and then becomes a pigmented cup-shaped cell with a foot that moves towards the ventral side of the sensory vesicle, while the ocellus remains embedded in the dorsal sensory vesicle epithelium. BPA did not inhibit foot formation but did prevent the detachment of the otolith from the dorsal sensory vesicle epithelium. Our data also suggests that the lower PC distance observed in BPA-treated embryos may also be due to a reduced expansion of the sensory vesicle lumen. Indeed, even though it was not quantified, we noticed that all bisphenols and ERR

antagonists also reduced the size of the sensory vesicle lumen. Because the ocellus and the otolith are located on opposite sides of the sensory vesicle, lumen expansion should participate in the separation of the two cells from each other. It has been shown that the ammonium transporter AMT-1a (Marino et al. 2007) and the ions transporter SLC26a (Deng et al. 2013) proteins are involved in sensory vesicle lumen expansion in ascidians. It would be thus interesting to assess if such genes are affected by BPA.

Strikingly, exposure of ascidian embryos to the BPA analogues BPE and BPF also inhibited pigmentation and the otolith movement towards the ventral side of the sensory vesicle. Such otolith phenotype seems to be specific to bisphenols since exposure to the bisphenyl 2,2DPP had no effect on larvae sensory vesicle (neither pigmentation, neither otolith movement nor sensory vesicle lumen). Interestingly, in zebrafish more than 50% of the embryos exposed to 25 µM BPA displayed abnormal otoliths (Gibert et al. 2011), with a similar bisphenol-specificity effect (Tohmé et al. 2014), suggesting that, even if zebrafish and ascidian otoliths as structurally different, bisphenols may share a similar mode of action in both ascidians and fish,. Because BPA, BPE and BPF can bind ERR and not 2,2 DDP (due to the lack of hydroxyl groups on its phenyl rings (Okada et al. 2008; Starovoytov et al. 2014)), our data indicate that, like in zebrafish (Tohmé et al. 2014), BPA may impair otolith development by affecting ERR activity.

4.3. BPA may target ERR during otolith movement in ascidian larvae

Recent evidence demonstrates that BPA is a weak ligand for the estrogen receptor (ER) but high affinity ligand for the estrogen-related receptor gamma (ERRγ) (Liu et al. 2014). This possibility was explored in the ascidian embryo. Ascidian genome have only one gene coding for ERR, and no estrogen nor steroid receptors (Yagi et al. 2003).

Transcriptomic data indicates ERR expression only at stage 26 for *Ciona robusta* and *Phallusia mammillata* (*Aniseed* database). In other ascidian species, PCR analysis showed that in *Herdmania curvata* ERR is expressed from gastrula (st. 10) throughout development (Devine et al. 2002), while *Halocynthia roretzi* ERR is expressed only from eggs up to gastrula (Park et al. 2009). Transcriptomic data available for *C. robusta* and *P. mammillata* ERR and our present data about *P. mammillata* ERR are not in agreement with the referred studies, as we show here that ERR transcripts and protein are present only from larvae (st. 26). Strikingly, we found that *Pm*-ERR is expressed within the sensory vesicle, specifically around the PC, around the time when the otolith moves towards the ventral side of the sensory vesicle. Additionally, most of the aminoacids known to be crucial for BPA specific binding to human ERRγ (Takayanagi et al. 2006; Okada et al. 2008; Liu et al. 2014) are conserved in *Pm*-ERR (data not shown), further supporting the hypothesis that BPA might bind to *Pm*-ERR to impair PC differentiation.

Our pharmacological screen suggests that ERR may be involved in the effect of BPA on the ascidian otolith movement. Firstly, lack of effect with the vertebrate ER agonist β-Estradiol 3-benzoate (E2B) is consistent with the fact that no ER-like or GPER-like proteins can be found in the ascidian genome (Yagi et al. 2003; Kamesh et al. 2008). Secondly, ERR antagonists diethylstilbestrol (DES) and 4-hydroxytamoxifen (4OHT) significantly reduced the distance between the two pigmented cells, suggesting a blocked otolith movement just as with BPA. Moreover, DES and 4OHT were able to suppress *Halocynthia roretzi* ERR activity in a dose-dependent manner (Park et al. 2009). However, it is important to point out that our data is different from a recent study (Messinetti et al. 2018a). While we found that the BPA phenotype is recapitulated by ERR inhibition using two different ERR antagonists (DES and 4OHT), Messinetti and colleagues found that an ERR antagonist (4OHT) could partially rescue the phenotype induced by BPA. Such difference may lie in the different criteria used to select embryonic cultures (>80% normal embryos and >300 µm^2 PC area in our study). Thus, our study suggests that BPA targets *Pm*-ERR to block otolith movement within the ascidian sensory vesicle.

4.4. BPA pleiotropic action in ascidian larvae

Finally, even if ERR is involved, it is probably not the only target in ascidian larvae. As mentioned before, exposure of ascidian embryos to vertebrate ERR antagonists inhibited otolith movement in a similar way to BPA, but it did not reduce pigmentation as reported after BPA exposure. The effect of BPA on pigmentation may be attributed to a partial inhibition of tyrosinase enzymatic activity, as bisphenols can inhibit tyrosinase enzymatic activity (Ruzza et al. 2017). Nevertheless, complete inhibition of tyrosinase enzyme by PTU resulted in larvae with well-formed pigmented cells but no melanin inside their melanosomes (Dumollard,

Gomes personal observations), a phenotype that was never observed with BPA, even at higher doses. Therefore, we hypothesize that BPA affects ERR and may also partially affects tyrosinase activity.

In addition, it is also important to note that BPA is affecting the otolith movement (PC distance) twice stronger than vertebrate ERR antagonists (31% vs ~60%), suggesting that BPA may have a pleiotropic action by targeting other nuclear receptors. Indeed, vertebrate Pregnane X Receptor (PXR), Thyroid Receptor (TR) and Peroxisome Proliferator-Activated Receptor (PPAR) have been shown to bind BPA (Moriyama et al. 2002; Sui et al. 2012; Delfosse et al. 2014; Ahmed and Atlas 2016) and ascidian orthologs are expressed in or near the larval brain during PC development (Gomes et al. 2019). Furthermore, ascidian PXR/VDRα has been shown to bind BPA (*Ciona robusta*, K_d: 5 µM) (Richter and Fidler, 2015). Receptor-ligand assays testing different ascidian NRs would be of greatest interest to characterize more in detail the multiple targets of BPA in ascidians that support its neurodevelopmental toxicity.

5. Conclusion

In this manuscript we show that BPA affects pigmentation and otolith movement in the brain of an invertebrate chordate species, the ascidian *Phallusia mammillata*. Because pigmented cells are part of the brain of the ascidian larvae, we demonstrate here that BPA induces neurodevelopmental toxicity to *P. mammillata* embryos.

We describe here for the first time the otolith formation and its movement towards the ventral side of the ascidian sensory vesicle. The expression of the nuclear receptor ERR during PC development, as well as the pharmacological approach, supports the hypothesis that ERR is involved in BPA neurodevelopmental toxicity, i.e., *Pm*-ERR may be involved in the otolith movement within the sensory vesicle. Because ERR antagonists did not affect the pigmentation process, the reduction of pigmentation induced by BPA is most likely controlled by other pathways. The potential binding of BPA to *P. mammillata* ERR, as well as the involvement of other nuclear receptors (PPAR, PXR and TR) in BPA neurodevelopmental toxicity is now being investigated in our laboratory.

Supplementary data

Supplementary figures are provided after the manuscript. Supplementary videos can be visualized from the following link: https://omero.france-bioinformatique.fr/omero/webclient/?show=dataset-2177

Acknowledgements

The authors would like to thank Filomena Ristoratore and Alberto Stolfi for kindly providing ascidian tyrosinase-related protein and ßγCrystallin promoters, respectively. Furthermore, the authors would like to thank Laurent Gilletta and Régis Lasbleiz and the *Centre de Ressources Biologiques Marines* of the *Institut de la Mer de Villefranche* (*CRBM - IMEV*) that is supported by *EMBRC-France*, whose French state funds are managed by the *Agence Nationale de la Recherche* (ANR) within the "*Investissement d'Avenir*" program (ANR-10-INBS-02). The experiments reported in this study were financed by an ANR grant (*Marine-EmbryoTox* project, ANR-14-OHRI-0009-01-1). Ievgeniia Gazo thanks to the Ministry of Education, Youth and Sports of the Czech Republic and projects CENAKVA (LM2018099) and Reproductive and Genetic Procedures for Preserving Fish Biodiversity and Aquaculture (CZ.02.1.01/0.0/0.0/16_025/0007370).

Competing interests

The authors have no competing interest to declare.

References

Abitua PB, Wagner E, Navarrete IA, Levine M. 2012. Identification of a rudimentary neural crest in a non-vertebrate chordate. Whitacre DM, editor. Nature. 492:104–108. doi:10.1016/j.biotechadv.2011.08.021.Secreted.

Acconcia F, Pallottini V, Marino M. 2015. Molecular mechanisms of action of BPA. Dose-Response. 13(4):1–9. doi:10.1177/1559325815610582.

Ahmed S, Atlas E. 2016. Bisphenol S- and bisphenol A-induced adipogenesis of murine preadipocytes occurs through direct peroxisome proliferator-activated receptor gamma activation. Int J Obes. 40(10):1566–1573. doi:10.1038/ijo.2016.95.

Allard P, Colaiacovo MP. 2010. Bisphenol A impairs the double-strand break repair machinery in the germline and causes chromosome abnormalities. Proc Natl Acad Sci. 107(47):20405–20410. doi:10.1073/pnas.1010386107.

Braun JM. 2017. Early-life exposure to EDCs: Role in childhood obesity and neurodevelopment. Nat Rev Endocrinol. 13(3):161–173. doi:10.1038/nrendo.2016.186.

Canesi L, Fabbri E. 2015. Environmental effects of BPA: Focus on aquatic species. Dose-Response. 13(3). doi:10.1177/1559325815598304.

Caracciolo A, Gesualdo I, Branno M, Aniello F, Di Lauro R, Palumbo A. 1997. Specific cellular localization of tyrosinase mRNA during Ciona intestinalis larval development. Dev Growth Differ. 39:437–444.

Delfosse V, Grimaldi M, le Maire A, Bourguet W, Balaguer P. 2014. Nuclear Receptor Profiling of Bisphenol-A and Its Halogenated Analogues. 1st ed. Elsevier Inc.

Deng W, Nies F, Feuer A, Bo I. 2013. Anion translocation through an Slc26 transporter mediates lumen expansion during tubulogenesis. doi:10.1073/pnas.1220884110/-/DCSupplemental.www.pnas.org/cgi/doi/10.1073/pnas.1220884110.

Devine C, Hinman VF, Degnan BM. 2002. Evolution and developmental expression of nuclear receptor genes in the ascidian Herdmania. Int J Dev Biol. 46:687–692.

Dilly N. 1962. Studies on the receptors in the cerebral vesicle of the ascidian tadpole: 1. The otolith. Q J Microsc Sci. 103(3):393–398. doi:10.1007/BF00321477.

Dilly N. 1964. Studies on the receptors in the cerebral vesicle of the ascidian tadpole: 2. The ocellus. Q J Microsc Sci. 105(1):13–20. doi:10.1007/BF00321477.

Dumollard R, Gazo I, Gomes IDL, Besnardeau L, McDougall A. 2017. Ascidians: An Emerging Marine Model for Drug Discovery and Screening. Curr Top Med Chem. 17:1–15. doi:10.2174/1568026617666170130.

Esposito R, Racioppi C, Pezzotti MR, Branno M, Locascio a., Ristoratore F, Spagnuolo a. 2015. The ascidian pigmented sensory organs: structures and developmental programs. Genesis. 53(November 2014):15–33. doi:10.1002/dvg.22836.

Flint S, Markle T, Thompson S, Wallace E. 2012. Bisphenol A exposure, effects, and policy: a wildlife perspective. J Environ Manage. 104:19–34. doi:10.1016/j.jenvman.2012.03.021. [accessed 2012 Nov 4]. http://www.ncbi.nlm.nih.gov/pubmed/22481365.

George O, Bryant BK, Chinnasamy R, Corona C, Arterburn JB, Shuster CB. 2008. Bisphenol A directly targets tubulin to disrupt spindle organization in embryonic and somatic cells. ACS Chem Biol. 20(3):123–132.

Gibert Y, Sassi-Messai S, Fini J-B, Bernard L, Zalko D, Cravedi J-P, Balaguer P, Andersson-Lendahl M, Demeneix B, Laudet V. 2011. Bisphenol A induces otolith malformations during vertebrate embryogenesis. BMC Dev Biol. 11(1):4. doi:10.1186/1471-213X-11-4.

Heyer DB, Meredith RM. 2017. Environmental toxicology: Sensitive periods of development and neurodevelopmental disorders. Neurotoxicology. 58:23–41. doi:10.1016/j.neuro.2016.10.017.

Holzer G, Markov G V., Laudet V. 2017. Evolution of Nuclear Receptors and Ligand Signaling: Toward a Soft Key–Lock Model? 1st ed. Elsevier Inc.

Hotta K, Mitsuhara K, Takahashi H, Inaba K, Oka K, Gojobori T, Ikeo K. 2007. A web-based interactive developmental table for the Ascidian Ciona intestinalis, including 3D real-image embryo reconstructions: I. From fertilized egg to hatching larva. Dev Dyn. 236:1790–1805. doi:10.1002/dvdy.21188.

Hudson C. 2016. The central nervous system of ascidian larvae. WIREs Dev Biol. doi:10.1002/wdev.239.

Hunt PA, Koehler KE, Susiarjo M, Hodges CA, Ilagan A, Voigt RC, Thomas S, Thomas BF, Hassold TJ. 2003. Bisphenol A Exposure Causes Meiotic Aneuploidy in the Female Mouse. Curr Biol. 13:546–553. doi:10.1016/S.

Inadera H. 2015. Neurological effects of bisphenol A and its analogues. Int J Med Sci. 12(12):926–936. doi:10.7150/ijms.13267.

Kamesh N, Aradhyam GK, Manoj N. 2008. The repertoire of G protein-coupled receptors in the sea squirt Ciona intestinalis. BMC Evol Biol. 8(129):1–19. doi:10.1186/1471-2148-8-129.

Kaur K, Simon A, Chauhan V, Chauhan A. 2015. Effect of bisphenol A on Drosophila melanogaster behavior –

616 A new model for the studies on neurodevelopmental disorders. Behav Brain Res. 284:77–84.
617 doi:10.1016/j.bbr.2015.02.001.

618 Konno A, Kaizu M, Hotta K, Horie T, Sasakura Y, Ikeo K, Inaba K. 2010. Distribution and structural diversity of
619 cilia in tadpole larvae of the ascidian Ciona intestinalis. Dev Biol. 337(1):42–62.
620 doi:10.1016/j.ydbio.2009.10.012.

621 Krishnan A V, Stathis P, Permuth SF, Tokes L, Feldman D. 1993. Bisphenol-A: an estrogenic substance is
622 released from polycarbonate flasks during autoclaving. Endocrinology. 132(6):2279–2286.

623 Liu X, Matsushima A, Shimohigashi M, Shimohigashi Y. 2014. A characteristic back support structure in the
624 bisphenol A-binding pocket in the human nuclear receptor ERRγ. PLoS One. 9(6).
625 doi:10.1371/journal.pone.0101252.

626 Mackay H, Abizaid A. 2018. A plurality of molecular targets: The receptor ecosystem for bisphenol-A (BPA).
627 Horm Behav. 101:59–67. doi:10.1016/j.yhbeh.2017.11.001.

628 Marino R, Melillo D, Filippo MDI, Yamada A, Pinto MR, Santis RDE, Brown ER, Matassi G. 2007. Ammonium
629 Channel Expression Is Essential for Brain Development and Function in the Larva of Ciona intestinalis. J
630 Comp Neurol. 503:135–147. doi:10.1002/cne.

631 Markov G V., Laudet V. 2011. Origin and evolution of the ligand-binding ability of nuclear receptors. Mol Cell
632 Endocrinol. 334(1–2):21–30. doi:10.1016/j.mce.2010.10.017.

633 Matsushima A, Ryan K, Shimohigashi Y, Meinertzhagen I a. 2013. An endocrine disruptor, bisphenol A,
634 affects development in the protochordate Ciona intestinalis: Hatching rates and swimming behavior alter in a
635 dose-dependent manner. Environ Pollut. 173:257–263. doi:10.1016/j.envpol.2012.10.015.

636 McDougall A, Chenevert J, Pruliere G, Costache V, Hebras C, Salez G, Dumollard R. 2015. Centrosomes and
637 spindles in ascidian embryos and eggs. Elsevier.

638 Mersha MD, Patel BM, Patel D, Richardson BN, Dhillon HS. 2015. Effects of BPA and BPS exposure limited to
639 early embryogenesis persist to impair non-associative learning in adults. Behav Brain Funct. 11(27):1–5.
640 doi:10.1186/s12993-015-0071-y.

641 Messinetti S, Mercurio S, Pennati R. 2018a. Effects of bisphenol A on the development of pigmented organs in
642 the ascidian *Phallusia mammillata*. Invertebr Biol.(September):1–10. doi:10.1111/ivb.12231.

643 Messinetti S, Mercurio S, Pennati R. 2018b. Bisphenol A affects neural development of the ascidian *Ciona*
644 *robusta*. J Exp Zool Part A Ecol Integr Physiol.(August):1–12. doi:10.1002/jez.2230.

645 Moriyama K, Tagami T, Akamizu T, Usui T, Saijo M, Kanamoto N, Hataya Y, Shimatsu A, Kuzuya H, Nakao K.
646 2002. Thyroid hormone action is disrupted by bisphenol A as an antagonist. J Clin Endocrinol Metab.
647 87(11):5185–5190. doi:10.1210/jc.2002-020209.

648 Murata M, Kang J. 2017. Bisphenol A (BPA) and cell signaling pathways. Biotechnol Adv.(August):0–1.
649 doi:10.1016/j.biotechadv.2017.12.002.

650 Mustieles V, Perez-Lobato R, Olea N, Fernandez MF. 2015. Bisphenol A: Human exposure and
651 neurobehavior. Neurotoxicology. 49:174–184. doi:10.1016/j.neuro.2015.06.002.

652 Nesan D, Sewell LC, Kurrasch DM. 2017. Opening the black box of endocrine disruption of brain
653 development: Lessons from the characterization of Bisphenol A. Horm Behav.:1–15.
654 doi:10.1016/j.yhbeh.2017.12.001.

655 Nishida H, Satoh N. 1989. Determination and regulation in the pigment cell lineage of the ascidian embryo.
656 Dev Biol. 132(2):355–67. doi:10.1016/0012-1606(89)90232-7.

657 Okada H, Tokunaga T, Liu X, Takayanagi S, Matsushima A, Shimohigashi Y. 2008. Direct evidence revealing
658 structural elements essential for the high binding ability of bisphenol a to human estrogen-related receptor
659 gamma. Environ Health Perspect. 116(1):32–38. doi:10.1289/ehp.10587.

660 Ozlem çakal A, Hatice P. 2007. Effects of Bisphenol A on the Embryonic Development of Sea Urchin
661 (Paracentrotus lividus). Environ Toxicol. 23:387–392. doi:10.1002/tox.

662 Paix A, Yamada L, Dru P, Lecordier H, Pruliere G, Chenevert J, Satoh N, Sardet C. 2009. Cortical anchorages
663 and cell type segregations of maternal postplasmic/PEM RNAs in ascidians. Dev Biol. 336(1):96–111.
664 doi:10.1016/j.ydbio.2009.09.001.

665 Park W, Kim GJ, Choi HS, Vanacker JM, Sohn YC. 2009. Conserved properties of a urochordate estrogen

receptor-related receptor (ERR) with mammalian ERRalpha. Biochim Biophys Acta. 1789(2):125–134. doi:10.1016/j.bbagrm.2008.08.011.

Racioppi C, Kamal AK, Razy-Krajka F, Gambardella G, Zanetti L, di Bernardo D, Sanges R, Christiaen L a., Ristoratore F. 2014. Fibroblast growth factor signalling controls nervous system patterning and pigment cell formation in Ciona intestinalis. Nat Commun. 5:4830. doi:10.1038/ncomms5830.

Ruzza P, Serra PA, Fabbri D, Dettori MA, Rocchitta G, Delogu G. 2017. Hydroxylated biphenyls as tyrosinase inhibitor: A spectrophotometric and electrochemical study. Eur J Med Chem. 126:1034–1038. doi:10.1016/j.ejmech.2016.12.028.

Ryan K, Lu Z, Meinertzhagen IA. 2016. The CNS connectome of a tadpole larva of Ciona intestinalis (L.) highlights sidedness in the brain of a chordate sibling. Elife. 5:1–34. doi:10.7554/eLife.16962.

Sakurai D, Goda M, Kohmura Y, Horie T, Iwamoto H, Ohtsuki H, Tsuda M. 2004. The role of pigment cells in the brain of ascidian larva. J Comp Neurol. 475(1):70–82. doi:10.1002/cne.20142.

Sardet C, McDougall A, Yasuo H, Chenevert J, Pruliere G, Dumollard R, Hudson C, Hebras C, Nguyen N Le, Paix A. 2011. Embryological Methods in Ascidians: The Villefranche-sur-Mer Protocols. In: Vertebrate Embryogenesis, Methods in Molecular Biology. Vol. 770. p. 365–400.

Schug T, Johnson AF, Birnbaum LS, Colborn T, Guillette LJ, Crews DP, Collins T, Soto AM, vom Saal FS, McLachlan JA, et al. 2016. Endocrine Disruptors: Past Lessons and Future Directions. Mol Endocrinol. 30(8):833–847. doi:10.1210/me.2016-1096.

Starovoytov ON, Liu Y, Tan L, Yang S. 2014. Effects of the Hydroxyl Group on Phenyl Based Ligand/ERRγ Protein Binding. Chem Res Toxicol. 27:1371–1379.

Stolfi A, Christiaen L. 2012. Genetic and genomic toolbox of the Chordate Ciona intestinalis. Genetics. 192(1):55–66. doi:10.1534/genetics.112.140590.

Sui Y, Ai N, Park SH, Rios-Pilier J, Perkins JT, Welsh WJ, Zhou C. 2012. Bisphenol A and its analogues activate human pregnane X receptor. Environ Health Perspect. 120(3):399–405. doi:10.1289/ehp.1104426.

Takayanagi S, Tokunaga T, Liu X, Okada H, Matsushima A, Shimohigashi Y. 2006. Endocrine disruptor bisphenol A strongly binds to human estrogen-related receptor gamma (ERRg) with high constitutive activity. Toxicol Lett. 167(2):95–105. doi:10.1016/j.toxlet.2006.08.012.

Tohmé M, Prud'Homme SM, Boulahtouf A, Samarut E, Brunet F, Bernard L, Bourguet W, Gibert Y, Balaguer P, Laudet V. 2014. Estrogen-related receptor γ is an in vivo receptor of bisphenol A. FASEB J. 28:3124–3133. doi:10.1096/fj.13-240465.

Tse WKF, Yeung BHY, Wan HT, Wong CKC. 2013. Early embryogenesis in zebrafish is affected by bisphenol A exposure. Biol Open. 2:466–71. doi:10.1242/bio.20134283.

Wasmeier C, Hume AN, Bolasco G, Seabra MC. 2008. Melanosomes at a glance. J Cell Sci. 121(24):3995–3999. doi:10.1242/jcs.040667.

Whittaker JR. 1966. An analysis of melanogenesis in differentiating pigment cells of ascidian embryos. Dev Biol. 14:1–39. doi:10.1016/0012-1606(66)90003-0.

Yagi K, Satou Y, Mazet F, Shimeld SM, Degnan B, Rokhsar D, Levine M, Kohara Y, Satoh N. 2003. A genomewide survey of developmentally relevant genes in Ciona intestinalis. III. Genes for Fox, ETS, nuclear receptors and NFKB. Dev Genes Evol. 213:235–244. doi:10.1007/s00427-003-0322-z.

Figure 1. Bisphenol A is toxic to *Phallusia mammillata* embryos in a dose-dependent manner. Embryos were exposed to different concentrations of Bisphenol A (BPA) from 1-cell stage, and three different phenotypes were assessed: *normal*, for larvae with elongated trunk and straight tail (white bars), *malformed* for larvae showing deformed trunk and/or bent tails (grey bars) and *not developed* for embryos displaying arrested development (black bars). Concentrations higher than 10µM significantly induced malformations. Concentrations higher than 20 µM significantly arrested development. The median effective (EC_{50}) and lethal (LC_{50}) concentrations are shown.

Figure 2. Bisphenol A disrupts pigment cell development in *Phallusia mammillata*. (A) Timecourse of pigment cell (PC) development in non-exposed embryos. The first pigments arrive at stage 21 (black arrowhead, t0), with an increase of pigmentation at stage 22. At stage 23, two distinct pigment cells (PC) are visible, the otolith (Ot) and the ocellus (Oc) (pink and blue arrowheads, respectively). Sensory vesicle lumen (SVl) and adhesive palps (P) (orange and yellow arrowheads, respectively) are visible as well at stage 23. Strong pigmentation for both PC is visible at stage 24. At stage 25 the trunk (T) starts to elongate (white arrowhead). Finally, at stage 26 (t5h) the trunk of the larvae is elongated and show two distinct pigmented cells, as well as adhesive palps. The otolith is now isolated within the sensory vesicle lumen. Scale bars: 10µm. **(B) Timecourse of PC development in Bisphenol A (BPA) exposed embryos.** Embryos were exposed to 10µM BPA from stage 1. Resulting BPA-exposed embryos (stage 26, t5h) showed severe reduction of pigmentation and an inhibition of otolith movement, resulting in a reduced distance between otolith and ocellus. Sensory vesicle lumen also seem reduced but it was not quantified. Trunk elongation and palps formation seem unaffected. Scale bars: 10µm. **(C) Effect of BPA in *P. mammillata* larvae.** Embryos were exposed to BPA 10 µM and three endpoints were quantified: the area of both pigmented cells (PC area, μm^2), the distance between the pigmented cells (PC distance, µm) and the length and width of the trunk (Trunk L/W ratio). Data was normalized to the control (DMSO, 100%) and plotted in a radar chart. All the three endpoints were significantly different from the control (0.01% DMSO; ANOVA - *Dunnett's* test), with the PC area and PC distance being the most affected ones (reduced to 35% and 31%, respectively). Descriptive statistics are represented in table I. Scale bar of representative phenotype: 10µm. **(D) Window of sensitivity of *P. mammillata* embryos to BPA.** Embryos were exposed to BPA (10µM): 6 hours before fertilization (6hbf, from stage 0 to 1), 6 hours post fertilization (6hpf, from stage 1 to 10), before fertilization up to gastrula (from stage 0 to 10) and then at different developmental stages between stages 10 and 20. The PC area (μm^2) was assessed at stage 26, when pigmentation process is finished. Exposure to BPA from stage 1 to 26, as well as all exposures between stage 10 and 20 were significantly different from the control (0.01% DMSO; ANOVA - *Dunnett's* test; *** p-value<0,001). Each point represents one embryo (n≥50 embryos from three independent experiments).

Figure 3. Bisphenol specifically disrupt otolith movement towards the ventral side of the sensory vesicle. (A) Pigment cells development within the sensory vesicle. At stage 21, otolith cell (followed by *ßγ-Crystallin* promoter *pßγC::GFP*) is visible within the sensory vesicle. The sensory vesicle surrounds the lumen that results from neural tube closure. At later stages (st. 23, 25), the otolith develops a foot that will allow the cell to move towards the ventral side of the brain sensory vesicle. Scale bars are 50µm, except insets (15µm). **(B) Timelapse of otolith movement towards the ventral side of the sensory vesicle lumen.** At the beginning of the pigmentation, otolith cell is next to ocellus cell (st. 22). Later, the epithelium invaginates towards the ventral side of the sensory vesicle lumen (st. 23-25), allowing the otolith to move away from the ocellus. At the end, the otolith foot is ventral and pigments are dorsal within the otolith cell (st. 26). Scale bars: 10µm. **(C) Timelapse of otolith movement in the presence of BPA.** In BPA-exposed embryos (BPA 10µM), otolith cell is next to ocellus cell (st. 22) and the epithelium still invaginates (st. 23-25), however the otolith stays attached to the epithelium (st. 26) until the embryo metamorphoses (not shown). Besides reduced pigmentation and blocked otolith movement, the sensory vesicle lumen seems reduced as well when compared to the control. Scale bars: 10µm. Supplementary videos 1 and 2 of described timelapses (B and C) can be downloaded from http://lbdv-local.obs-vlfr.fr/~dumollard/.

Figure 4. Bisphenols, but not bisphenyl, specifically disrupt pigmentation and otolith movement towards the ventral side of the sensory vesicle. (A) Molecular structures of BPA, BPE, BPF and 2,2DPP. (B-F) Comparison of otolith foot structure between non-exposed embryos (0.01% DMSO), and bisphenols and bisphenyl. In non-exposed larvae **(B: 0.01% DMSO)**, the otolith foot (purple dot) is attached to the ventral side of the sensory vesicle, and an accumulation of actin is observed. A similar otolith foot phenotype was also visible in larvae exposed to 2,2 DPP **(F)**. However, in larvae exposed to BPA **(C)**, BPE **(D)** and BPF **(E)**, the otolith foot is arrested on the posterior or even dorsal side of the sensory vesicle. For comparison, all larvae were exposed to 10µM of each drug with exception for 2,2 DPP that showed no otolith phenotype either at 10, 25 or 100 µM. Larvae were fixed and stained for actin and DNA (Phalloidin and Hoechst staining, respectively). *n*: nucleus, *f*: foot, *v*: ventral. All scale bars are 50µm (insets: 15µm).

Figure 5. *Phallusia mammillata* express an Estrogen-Related Receptor (ERR) in the ascidian larval sensory vesicle. (A) *Pm*-ERR mRNA spatial expression. *Pm*-ERR transcript was assessed by *in situ* hybridization and spatial

765 expression was only visible from stage 26. *Pm*-ERR mRNA is expressed within the sensory vesicle (SV), specifically
766 bellow the otolith, above the ocellus and between both pigment cells, also in the palps and in the trunk ganglion (Tg) (black
767 arrowheads). **(B) *Pm*-ERR promoter activity.** The promoter region of *Pm*-ERR, corresponding to 1.7kbp before the first
768 ATG, was cloned into a *H2B::Venus* reporter plasmid and injected in *P. mammillata* eggs. Two types of expression were
769 obtained: in the sensory vesicle and palps, or in the sensory vesicle and trunk ganglion (white arrowheads). **(C-D) *Pm*-**
770 **ERR protein expression. (C)** In order to study protein expression, a *Pm*-ERR antibody was raised and validated by
771 injecting eggs with exogenous ERR mRNA (ERR::Venus). **(D)** *Pm*-ERR protein expression was assessed in *P. mammillata*
772 eggs, neurulas (st. 15), late tailbuds (st. 21) and larvae (st. 26), showing its presence only from stage 26 (N=6), in a similar
773 way as mRNA and promoter results. Tubulin antibody was used as control. Scale bars: 50µm.
774
775 **Figure 6. Estrogen-related receptor (ERR) antagonists partially phenocopied BPA neurodevelopmental toxicity,**
776 **but not Estrogen Receptor (ER) agonist. (A-C) Three endpoint-radar charts for comparison between BPA and E2B,**
777 **DES and 4OHT.** For phenotype comparison, the following endpoints were measured: the area of pigmented cells (PC
778 area, μm^2), the distance between pigmented cells (PC distance, µm) and the length and width of the trunk (Trunk L/W
779 ratio). Graphs are normalized to the control (DMSO, 100%). Embryos exposed to the ER agonist β-estradiol 3-benzoate
780 **(E2B, A)** had no effect on development. Embryos exposed to the ERR antagonist diethylstilbestrol **(DES, B)** and the ERR
781 antagonist 4-hydroxytamoxifen **(4OHT, C)** severely affected PC distance, as well as mild reduction of trunk elongation
782 ($N \geq 3$). Respective molecular structures and representative phenotype pictures are provided (scale bars: 20µm). Please
783 refer to the table I for the descriptive statistics.
784
785 **Figure S1. Bisphenol A induces genotoxicity at high doses.** *P. mammillata* eggs were fertilized and immediately
786 exposed to BPA 40µM. Embryos were then fixed at the first mitosis (64min after fertilization) and stained for microtubules
787 (anti-DM1α, green) and DNA (DAPI, blue). While most of non-exposed embryos (0.01% DMSO) showed a well-formed
788 mitotic spindle, high dose of BPA blocked embryos to exit meiosis before mitosis, displaying both mitotic and meiotic
789 spindles. Scale bars: 50µm.
790
791 **Figure S2. Bisphenol A does not affect *P. mammillata* pigment cell (PC) nor central nervous system (CNS)**
792 **specification lineages. (A) BPA phenotype is different from PTU and UO126.** Embryos were exposed to the
793 tyrosinase enzyme inhibitor phenylthiourea (PTU, 200µM) at stage 1, and to the MAPK inhibitor UO126 (4µM) at stages 16
794 and 18 (corresponding to before and after the last MAPK signal induction for PC specification, respectively). PTU
795 completely abolished pigmentation (melanin) but melanosomes structures are intact. Exposure to UO126 at stage 16 also
796 abolished pigmentation, but not when embryos were exposed to UO126 at stage 18. BPA still induced the phenotype
797 (reduced pigmentation and otolith blocked movement) even when incubated at stage 22, but not at stage 24. Scale bars
798 are 50µm, except insets (15µm). **(B-C) Spatial expression of PC and CNS specification genes are not affected by**
799 **BPA.** The mRNA of genes driving/involved in **(B)** PC (*Opsin*, *Pax6*, *Rab32/38*, *Tyr*) and in **(C)** CNS (*Cnga*, *Coe*, *Eya*, *Islet*)
800 specification were assessed by *in situ* hybridization, in both non-exposed (WT) and BPA-exposed (10µM) embryos.
801 Expression does not seem to be affected by BPA. **(D) Cilia of the neurohypophysial duct and neural tube are not**
802 **affected by BPA.** Expression of acetylated tubulin, marker of the ascidian neurohypophysial duct and neural tube cilia,
803 was assessed by antibody staining, in both non-exposed (WT) and BPA-exposed (10µM) embryos. Expression does not
804 seem to be affected by BPA. Note: all embryos were exposed to drugs from 1-cell stage, unless specified. Scale bars are
805 50µm.
806
807

Table I. Descriptive statistics of radar charts. Raw data of each radar chart is provided. Data was analyzed based on One-Way ANOVA. Because data did not follow a Gaussian distribution (normality test Shapiro-Wilk), data was analyzed using Kruskal-Wallis test followed by Dunnett's multiple comparison test (Dunn's MCT). * p-value<0.05; ** p-value<0.01; *** p-value<0.001.

PC area (µm2)	**n**	**Min**	**Max**	**Mean**	**Std**	**Dunn's MCT**	**% to the control**	**Adj p-value**	**Summary**
DMSO	486	188	636	382	82,8	-	-	-	-
BPA 10µM	255	0	361	122	83,5	DMSO vs. BPA 10µM	35	<,001	***
E2B 10µM	162	138	602	360	100	DMSO vs. E2B 10µM	94	0,881	ns
DES 1µM	144	171	557	384	68,3	DMSO vs. DES 1µM	101	>,999	ns
4-OHT 5µM	148	73,2	624	376	102	DMSO vs. 4-OHT 5µM	98	>,999	ns
4-OHT 10µM	105	150	672	398	107	DMSO vs. 4-OHT 10µM	105	>,999	ns

PC distance (µm)	**n**	**Min**	**Max**	**Mean**	**Std**	**Dunn's MCT**	**% to the control**	**Adj p-value**	**Summary**
DMSO	485	0	41,5	24,1	8,52	-	-	-	-
BPA 10µM	278	0	32,3	7	10,1	DMSO vs. BPA 10µM	31	<,001	***
E2B 10µM	161	0	36,7	22,1	9,28	DMSO vs. E2B 10µM	88	0,15	ns
DES 1µM	145	0	34,2	15,9	11,9	DMSO vs. DES 1µM	65	<,001	***
4-OHT 5µM	149	0	40	15,3	13,1	DMSO vs. 4-OHT 5µM	63	<,001	***
4-OHT 10µM	105	0	40,6	13,9	13,6	DMSO vs. 4-OHT 10µM	58	<,001	***

Trunk L/W ratio	**n**	**Min**	**Max**	**Mean**	**Std**	**Dunn's MCT**	**% to the control**	**Adj p-value**	**Summary**
DMSO	486	1,01	4,34	2,53	0,52	-	-	-	-
BPA 10µM	279	1,01	2,89	1,72	0,41	DMSO vs. BPA 10µM	70	<,001	***
E2B 10µM	162	1,21	3,5	2,5	0,4	DMSO vs. E2B 10µM	98	>,999	ns
DES 1µM	270	1,07	2,73	1,75	0,32	DMSO vs. DES 1µM	75	<,001	***
4-OHT 5µM	148	1,36	3,82	2,29	0,53	DMSO vs. 4-OHT 5µM	91	<,001	***
4-OHT 10µM	106	1,03	2,75	1,91	0,31	DMSO vs. 4-OHT 10µM	75	<,001	***

Figure 1

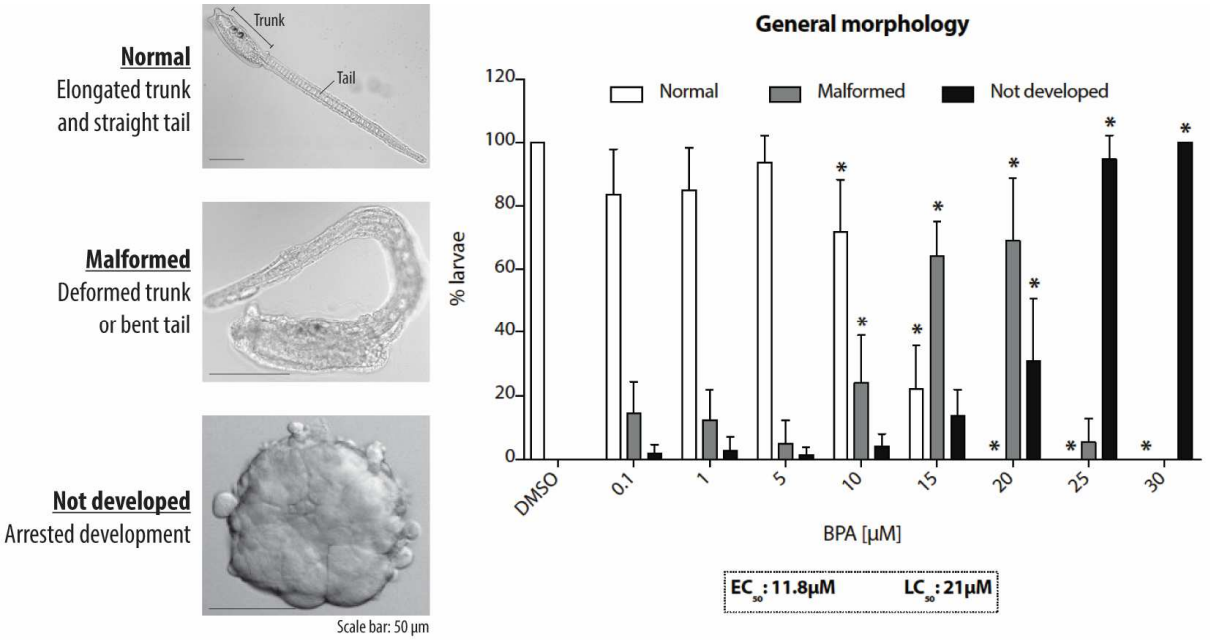
Normal
Elongated trunk
and straight tail
Trunk
Tail
Malformed
Deformed trunk
or bent tail
Not developed
Arrested development
Scale bar: 50 µm
General morphology
Normal
Malformed
Not developed
% larvae
120
100
80
60
40
20
0
DMSO
0.1
1
5
10
15
20
25
30
BPA [µM]
EC50: 11.8µM
LC50: 21µM

Figure 2

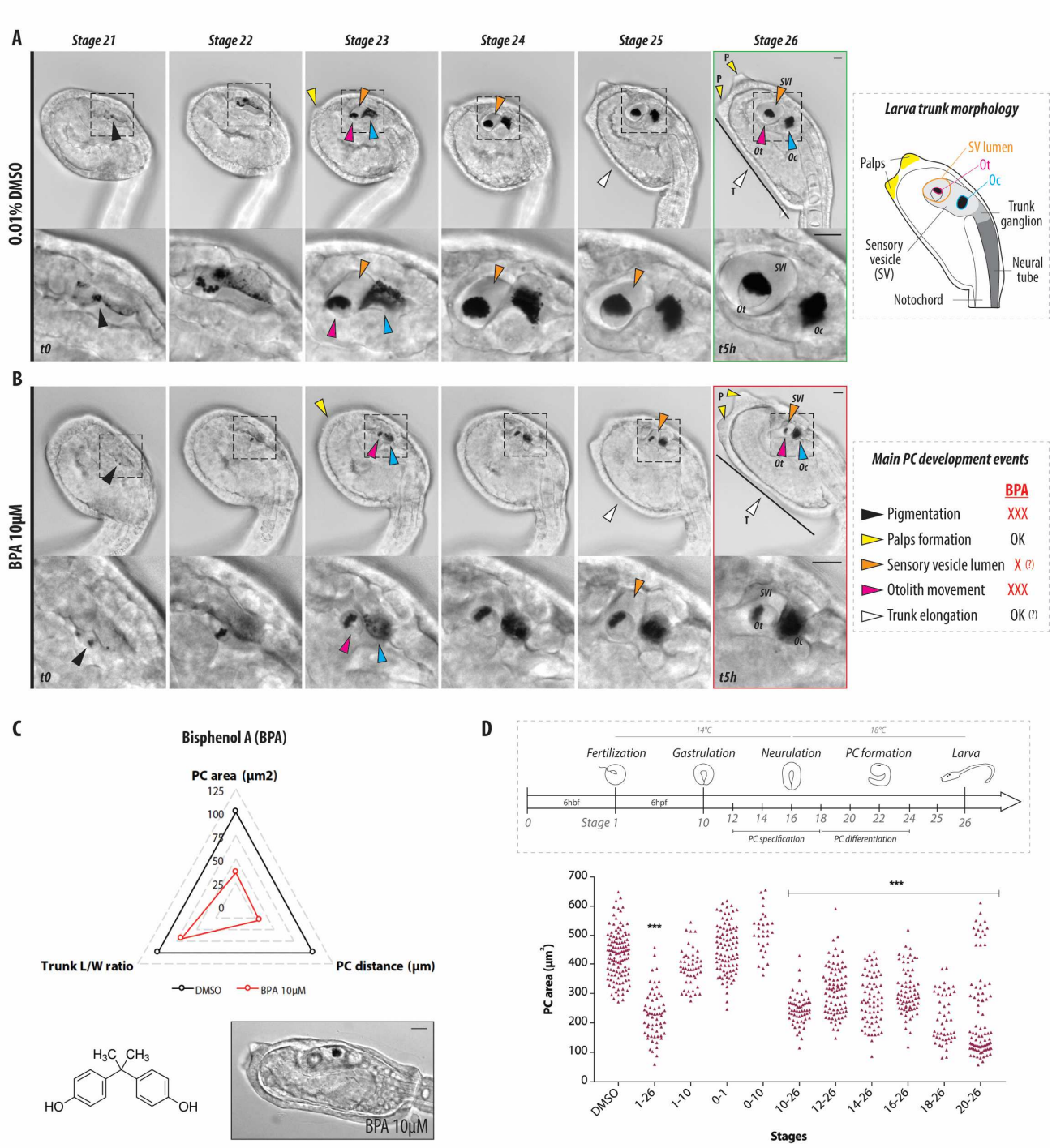
A
Stage 21
Stage 22
Stage 23
Stage 24
Stage 25
Stage 26
0.01% DMSO
t0
t5h
SVl
Ot
Oc
P
T
Larva trunk morphology
Palps
SV lumen
Ot
Oc
Trunk ganglion
Sensory vesicle (SV)
Neural tube
Notochord
B
BPA 10µM
Main PC development events
BPA
Pigmentation XXX
Palps formation OK
Sensory vesicle lumen X (?)
Otolith movement XXX
Trunk elongation OK (?)
C
Bisphenol A (BPA)
PC area (µm2)
125
100
75
50
25
0
Trunk L/W ratio
PC distance (µm)
DMSO
BPA 10µM
H3C CH3
HO
OH
BPA 10µM
D
14°C
18°C
Fertilization
Gastrulation
Neurulation
PC formation
Larva
6hbf
6hpf
0
Stage 1
10
12
14
16
18
20
22
24
25
26
PC specification
PC differentiation
PC area (µm²)
700
600
500
400
300
200
100
0
***
***
DMSO
1-26
1-10
0-1
0-10
10-26
12-26
14-26
16-26
18-26
20-26
Stages

Figure 3

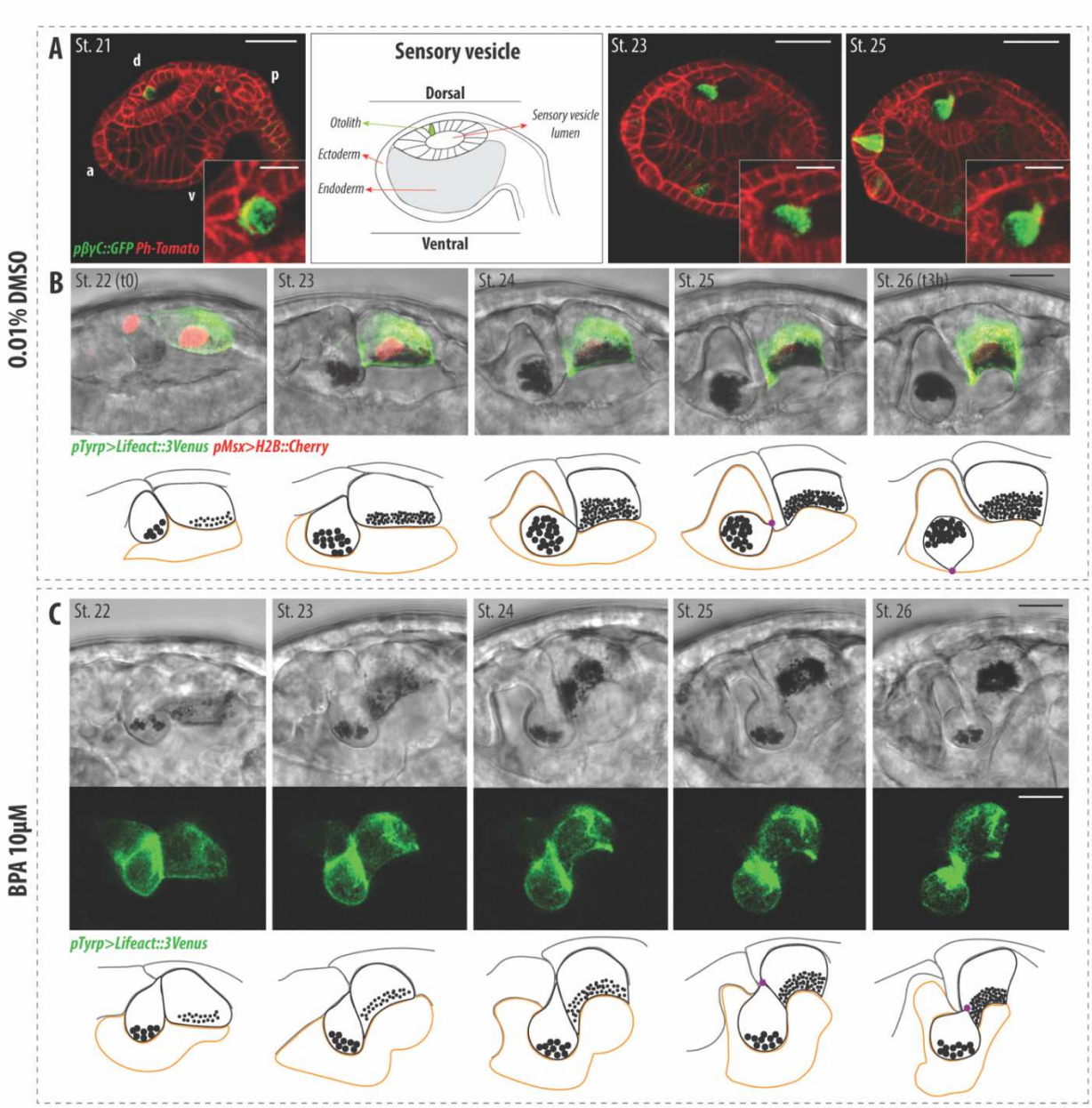
A
St. 21
d
p
a
v
pβγC::GFP Ph-Tomato
Sensory vesicle
Dorsal
Otolith
Sensory vesicle lumen
Ectoderm
Endoderm
Ventral
St. 23
St. 25
0.01% DMSO
B
St. 22 (t0)
St. 23
St. 24
St. 25
St. 26 (t3h)
pTyrp>Lifeact::3Venus pMsx>H2B::Cherry
C
St. 22
St. 23
St. 24
St. 25
St. 26
BPA 10µM
pTyrp>Lifeact::3Venus

Figure 4

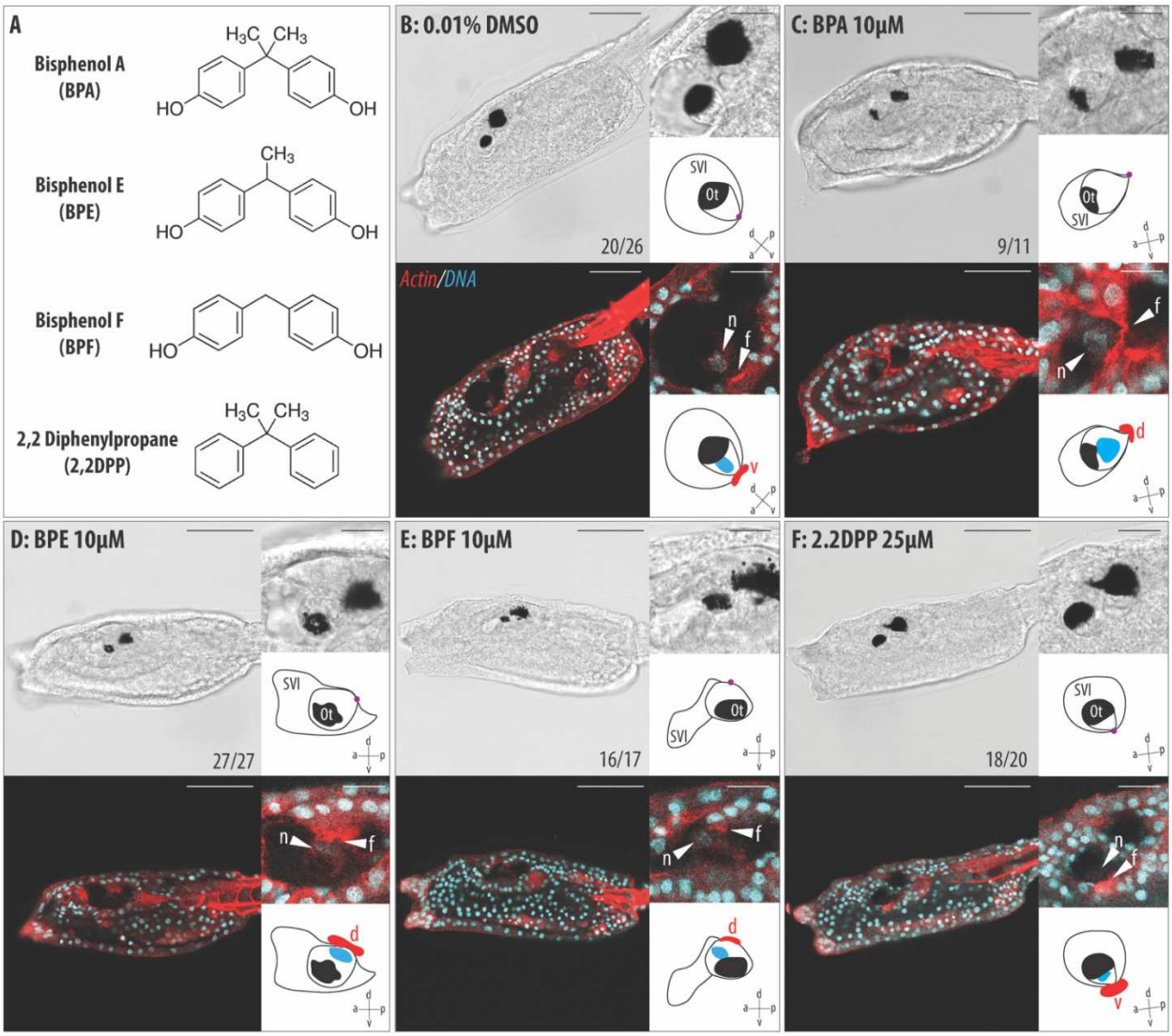
A
Bisphenol A (BPA)
Bisphenol E (BPE)
Bisphenol F (BPF)
2,2 Diphenylpropane (2,2DPP)
B: 0.01% DMSO
20/26
C: BPA 10µM
9/11
Actin/DNA
D: BPE 10µM
27/27
E: BPF 10µM
16/17
F: 2.2DPP 25µM
18/20
SVI
Ot
n
f
d
v

Figure 5

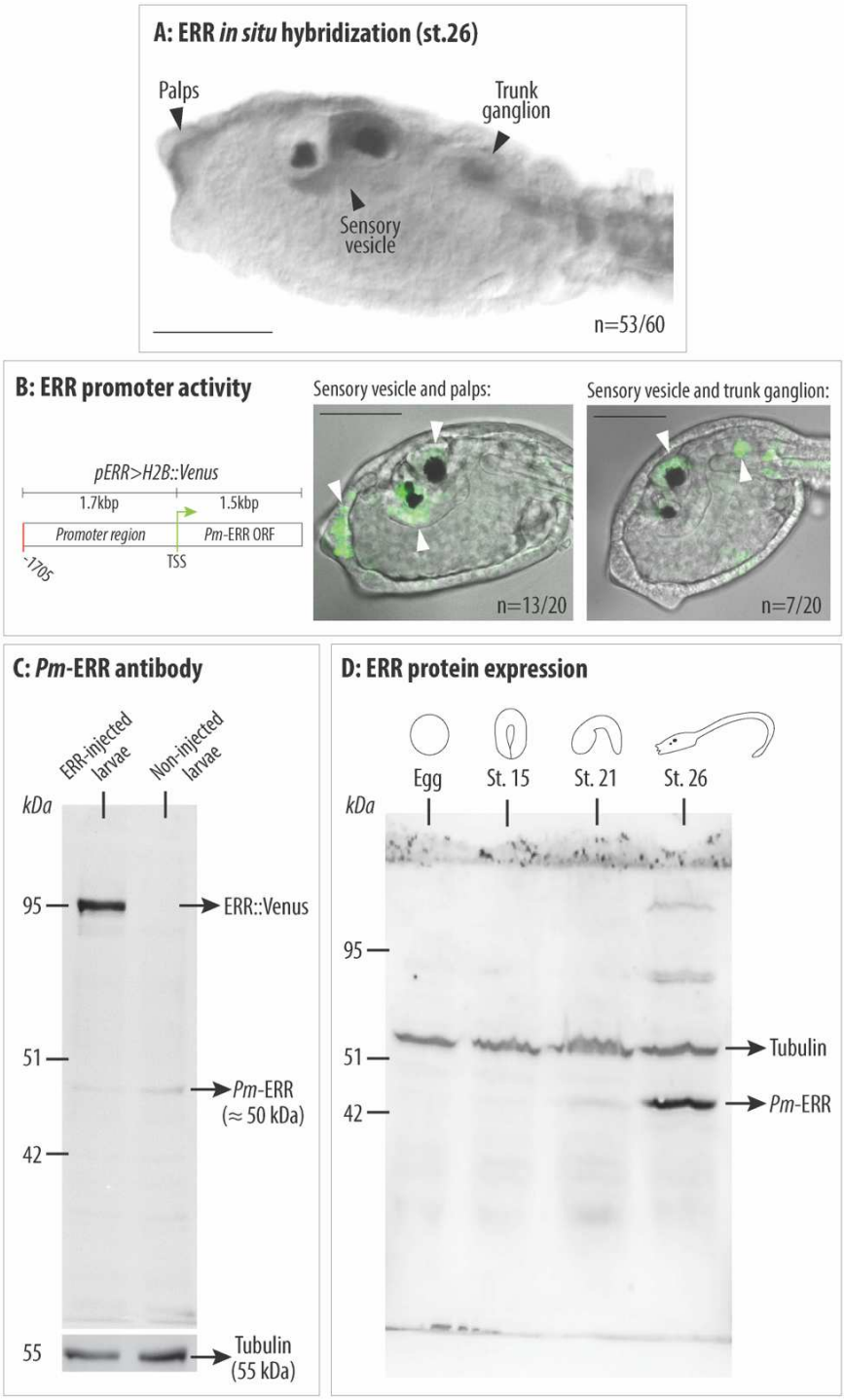
A: ERR *in situ* hybridization (st.26)
Palps
Trunk ganglion
Sensory vesicle
n=53/60
B: ERR promoter activity
pERR>H2B::Venus
1.7kbp
1.5kbp
Promoter region
Pm-ERR ORF
-1705
TSS
Sensory vesicle and palps:
n=13/20
Sensory vesicle and trunk ganglion:
n=7/20
C: Pm-ERR antibody
ERR-injected larvae
Non-injected larvae
kDa
95
51
42
55
ERR::Venus
Pm-ERR (≈ 50 kDa)
Tubulin (55 kDa)
D: ERR protein expression
Egg
St. 15
St. 21
St. 26
kDa
95
51
42
Tubulin
Pm-ERR

Figure 6

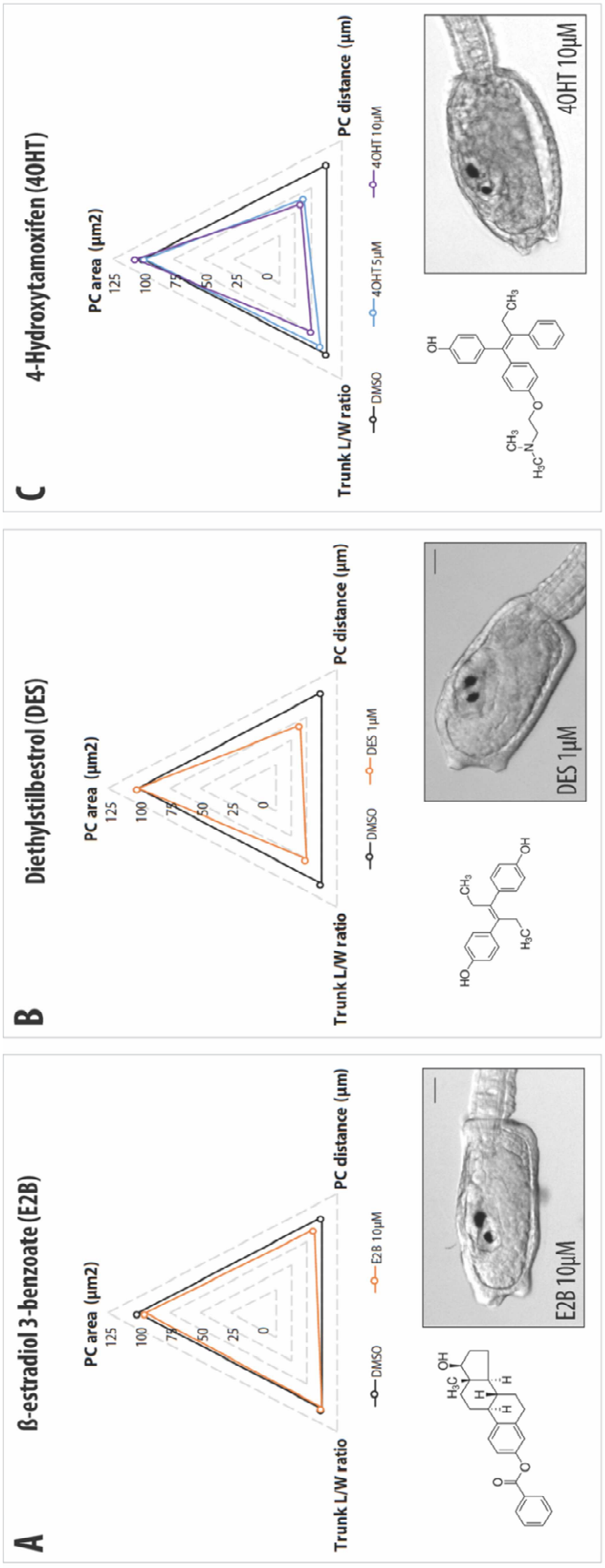
A
ß-estradiol 3-benzoate (E2B)
PC area (µm2)
125
100
75
50
25
0
PC distance (µm)
Trunk L/W ratio
DMSO
E2B 10µM
E2B 10µM
B
Diethylstilbestrol (DES)
PC area (µm2)
125
100
75
50
25
0
PC distance (µm)
Trunk L/W ratio
DMSO
DES 1µM
DES 1µM
C
4-Hydroxytamoxifen (4OHT)
PC area (µm2)
125
100
75
50
25
0
PC distance (µm)
Trunk L/W ratio
DMSO
4OHT 5µM
4OHT 10µM
4OHT 10µM

Figure S1

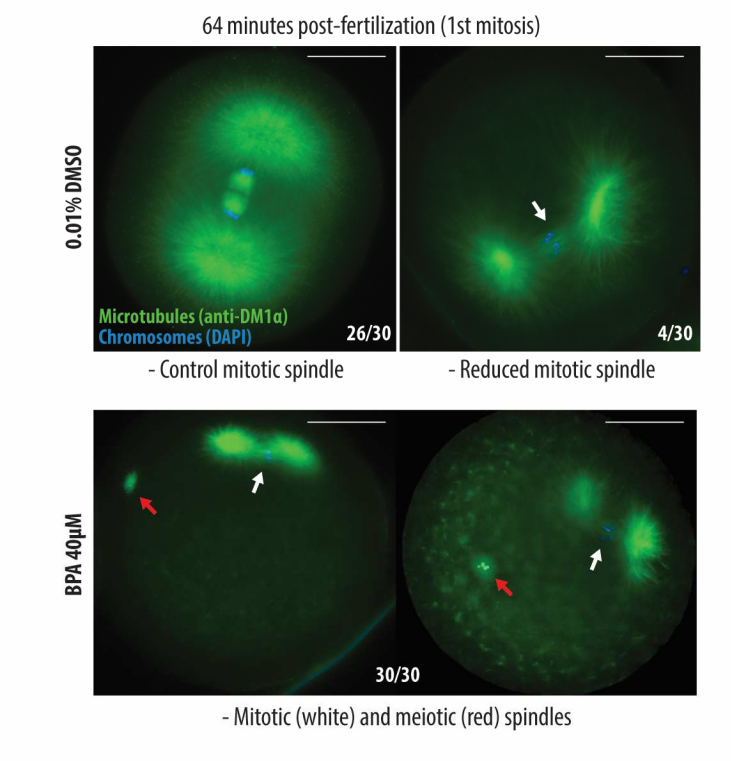
64 minutes post-fertilization (1st mitosis)
0.01% DMSO
Microtubules (anti-DM1α)
Chromosomes (DAPI)
26/30
4/30
- Control mitotic spindle
- Reduced mitotic spindle
BPA 40µM
30/30
- Mitotic (white) and meiotic (red) spindles

Figure S2

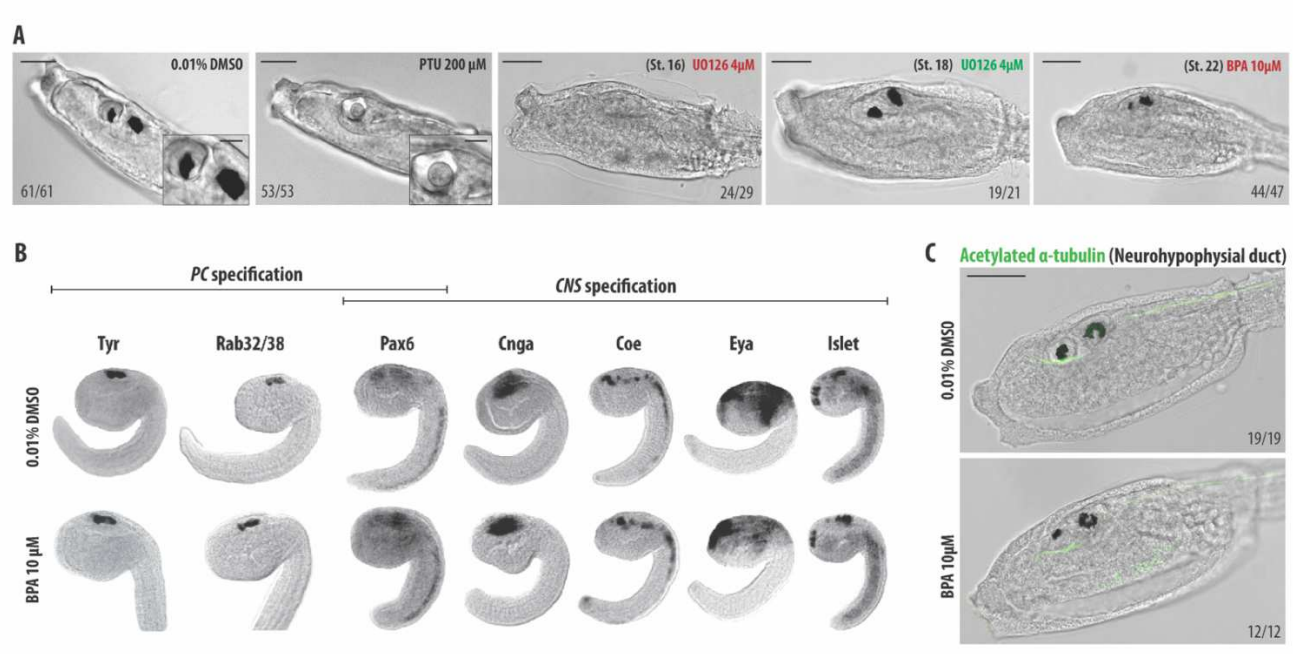
A
0.01% DMSO
61/61
PTU 200 µM
53/53
(St. 16) U0126 4µM
24/29
(St. 18) U0126 4µM
19/21
(St. 22) BPA 10µM
44/47
B
PC specification
CNS specification
Tyr
Rab32/38
Pax6
Cnga
Coe
Eya
Islet
0.01% DMSO
BPA 10 µM
C
Acetylated α-tubulin (Neurohypophysial duct)
0.01% DMSO
19/19
BPA 10µM
12/12